

10-13-1996

The Product of the *Saccharomyces Cerevisiae* RSS1 Gene, Identified as a High-Copy Suppressor of the Rat7-1 Temperature-Sensitive Allele of the RAT7/NUP159 Nucleoporin, is Required for Efficient mRNA Export


Veronica Del Priore
Dartmouth College

Christine A. Snay
Dartmouth College

Andre Bahr
University of Mainz

Charles N. Cole
Dartmouth College

Follow this and additional works at: <https://digitalcommons.dartmouth.edu/facoa>

 Part of the [Life Sciences Commons](#), and the [Medicine and Health Sciences Commons](#)

Recommended Citation

Del Priore, Veronica; Snay, Christine A.; Bahr, Andre; and Cole, Charles N., "The Product of the *Saccharomyces Cerevisiae* RSS1 Gene, Identified as a High-Copy Suppressor of the Rat7-1 Temperature-Sensitive Allele of the RAT7/NUP159 Nucleoporin, is Required for Efficient mRNA Export" (1996). *Open Dartmouth: Faculty Open Access Articles*. 3826.
<https://digitalcommons.dartmouth.edu/facoa/3826>

The Product of the *Saccharomyces cerevisiae* *RSS1* Gene, Identified as a High-Copy Suppressor of the *rat7-1* Temperature-sensitive Allele of the *RAT7/NUP159* Nucleoporin, Is Required for Efficient mRNA Export

Veronica Del Priore,* Christine A. Snay,* André Bahr,[†] and Charles N. Cole*[‡]

*Department of Biochemistry, Dartmouth Medical School, Hanover, New Hampshire 03755; and

[†]Institute of Molecular Genetics, University of Mainz, Mainz, Germany

Submitted April 18, 1996; Accepted July 24, 1996

Monitoring Editor: Randy W. Schekman

RAT7/NUP159 was identified previously in a screen for genes whose products are important for nucleocytoplasmic export of poly(A)⁺ RNA and encodes an essential nucleoporin. We report here the identification of *RSS1* (Rat Seven Suppressor) as a high-copy extragenic suppressor of the *rat7-1* temperature-sensitive allele. *Rss1p* encodes a novel essential protein of 538 amino acids, which contains an extended predicted coiled-coil domain and is located both at nuclear pore complexes (NPCs) and in the cytoplasm. *RSS1* is the first reported high-copy extragenic suppressor of a mutant nucleoporin. Overexpression of *Rss1p* partially suppresses the defects in nucleocytoplasmic export of poly(A)⁺ RNA, rRNA synthesis and processing, and nucleolar morphology seen in *rat7-1* cells shifted to the nonpermissive temperature of 37°C and, thus, restores these processes to levels adequate for growth at a rate approximately one-half that of wild-type cells. After a shift to 37°C, the mutant *Rat7-1p/Nup159-1p* is lost from the nuclear rim of *rat7-1* cells and NPCs, which are clustered together in these cells grown under permissive conditions become substantially less clustered. Overexpression of *Rss1p* did not result in retention of the mutant *Rat7-1p/Nup159-1p* in NPCs, but it did result in partial maintenance of the NPC-clustering phenotype seen in mutant cells. Depletion of *Rss1p* by placing the *RSS1* open reading frame (ORF) under control of the *GAL1* promoter led to cessation of growth and nuclear accumulation of poly(A)⁺ RNA without affecting nuclear protein import or nuclear pore complex distribution, suggesting that *RSS1* is directly involved in mRNA export. Because both *rat7-1* cells and cells depleted for *Rss1p* are defective in mRNA export, our data are consistent with both gene products playing essential roles in the process of mRNA export and suggest that *Rss1p* overexpression suppresses the growth defect of *rat7-1* cells at 37°C by acting to maintain mRNA export.

INTRODUCTION

The exchange of macromolecules between the nucleus and the cytoplasm is an essential process in eukaryotic

cells. After transcription and post-transcriptional RNA processing, mRNAs are transported to the cytoplasm through nuclear pore complexes where they function in protein synthesis. Initial approaches to investigate RNA export involved microinjection of RNA-coated gold particles into the nucleus of *Xenopus* oocytes,

[‡] Corresponding author.

which showed that poly(A)⁺ RNA, tRNA, and 5S rRNA can be exported efficiently and in a saturable manner (Dworetzky and Feldherr, 1988). Nucleocytoplasmic export of Balbiani ring granules, abundant and specific premessenger ribonucleoprotein particles (RNP) produced in the salivary glands of *Chironomus tentans*, has been shown by electron microscopy tomography to proceed through the central channel of the NPC (Mehlin *et al.*, 1992). These RNP particles change from a globular to a more linear conformation as they begin to translocate through NPCs, with the 5' end of the RNP particle moving through the NPC first (Mehlin *et al.*, 1992). Several proteins that mediate RNA transport have been identified in yeast. One of these proteins, called Npl3p, is closely related to mammalian hnRNP proteins and is known to shuttle between the nucleus and the cytoplasm (Flach *et al.*, 1994). Despite all these findings, the lack of an *in vitro* system to study RNA export has made it difficult to gain a complete understanding of this process and to identify all of the gene products this process requires.

Nuclear pore complexes (NPCs) form the only channels between nucleus and cytoplasm and are embedded in the nuclear envelope at places where the inner and outer nuclear membranes are fused. These complex structures, with a mass of ~125 mDa in metazoan cells and 65 mDa in *Saccharomyces cerevisiae*, are thought to contain at least 50 different polypeptide species (for review, Rout and Wentz, 1994; Davis, 1995; Doye and Hurt, 1995). From high-resolution electron microscopy image reconstruction, NPCs are thought to consist of a central spoke/ring assembly that is anchored in the nuclear envelope by transmembrane protein components of the NPC, a central transporter through which substrates move as they are actively translocated into or out of the nucleus, a basket-like structure located at the nucleoplasmic face of the NPC, and fibrils that emanate from the cytoplasmic face of the NPC (Maul, 1977; Unwin and Milligan, 1982; Richardson *et al.*, 1988; Allen and Douglas, 1989; Akey, 1990, 1991, 1995; Akey and Radermacher, 1993; Reichelt *et al.*, 1990; Jarnik and Aebi, 1991; Goldberg and Allen, 1992; Hinshaw *et al.*, 1992; Ris and Malecki, 1993). NPCs possess 9-nm channels through which solutes, ions, metabolites, and proteins smaller than 50 kDa move by passive diffusion. The transport of larger macromolecules, including proteins and ribonucleoproteins, is thought to use the transporter in the central channel of the NPC and requires both energy and specific signals within the transported macromolecule (for review, Elliot *et al.*, 1994; Fabre and Hurt, 1994; Davis, 1995; Izaurralde and Mattaj, 1995).

Approximately 20 yeast nucleoporins and a smaller number from metazoan cells have been identified by biochemical, immunochemical, and genetic approaches (for review, Doye and Hurt, 1995). On the

basis of their primary sequence, they fall into three broad classes. The first class consists of proteins with multiple repeats of short motifs that include GLFG, XFXFG, or XXFG. These repeats seem to interact with a multiprotein complex that contains a karyophilic protein to be imported into the nucleus and the heterodimeric receptor that recognizes nuclear localization sequences (NLSs). This receptor consists of Srp1p and Kap95p (Görlich *et al.*, 1995; Iovine *et al.*, 1995; Moroianu *et al.*, 1995; Rexach and Blobel, 1995). The second class of nucleoporins consists of a few with transmembrane domains that are thought to anchor the pore in the nuclear envelope (Wozniak *et al.*, 1989, 1994; Wozniak and Blobel, 1992; Greber *et al.*, 1990). The third class consists of proteins that lack peptide repeats and are not transmembrane proteins. Many NPC proteins contain potential coiled-coil domains that could provide a basis for interactions among NPC polypeptides.

Through a screen for temperature-sensitive mutants of *S. cerevisiae* that accumulate poly(A)⁺ RNA in their nuclei after a shift to the nonpermissive temperature, we isolated mutant alleles of *RAT2/NUP120*, *RAT3/NUP133*, *RAT7/NUP159*, *RAT9/NUP85*, and *NUP145* (Gorsch *et al.*, 1995; Heath *et al.*, 1995; Li *et al.*, 1995; Goldstein *et al.*, 1996; Dockendorff and Cole, unpublished results). In cells carrying the *rat7-1* allele of *RAT7/NUP159*, poly(A)⁺ RNA accumulates very rapidly in the nuclei after a shift to the nonpermissive temperature, but there is no apparent defect in nuclear protein import. *rat7-1* mutant cells show clustering of NPCs at 23°C and also have defects in nucleolar function and structure at 37°C (Gorsch *et al.*, 1995; Heath *et al.*, 1995; Kraemer *et al.*, 1995). When *rat7-1* cells are shifted to 37°C, *Rat7-1p* is lost from NPCs, and the pores rapidly become less clustered (Gorsch *et al.*, 1995). By immunoelectron microscopy, *Rat7p/Nup159p* has been localized to a position at the cytoplasmic periphery of the NPC, and it may be a component of the cytoplasmic fibrils (Kraemer *et al.*, 1995).

We conducted a screen for high-copy suppressors of the *ts* growth defect of the *rat7-1* strain. The *RAT7/NUP159* gene and plasmids encoding the carboxyl portion of *Rat7p/Nup159p* were isolated repeatedly. The most frequently isolated extragenic suppressor has been named *RSS1* (Rat Seven Suppressor). *Rss1p* encodes a novel protein of 538 amino acids, which contains an extended predicted coiled-coil domain, and is located both at NPCs and in the cytoplasm. The presence of high-copy *RSS1* permitted the *rat7-1* strain to grow as well at 37°C as it does in the absence of the suppressor at 23°C, but it did not restore wild-type growth properties to *rat7-1* cells. *RSS1* partially suppressed the nucleolar defects and the RNA export block of *rat7-1* cells, but the mutant *Rat7-1p/Nup159-1p* was still lost from nuclear pores when cells were shifted to the nonpermissive temperature. Inter-

estingly, in the presence of high-copy *RSS1*, NPCs remained partially clustered in *rat7-1* cells shifted to the nonpermissive temperature. When the *RSS1* open reading frame (ORF) was placed under control of a *GAL1* promoter, cells were able to grow only when the *GAL1* promoter was active. When *Rss1p* was depleted by transferring these cells to glucose-containing media, almost all of the cells developed a defect in the export of poly(A)⁺ RNA within 9 h but did not show a defect in nuclear protein import, suggesting that *Rss1p* plays a primary role in RNA export.

MATERIALS AND METHODS

Yeast Strains, Cell Culture, and Genetic Methods

Yeast strains used in this study are listed in Table 1, and the plasmids used are listed in Table 2. Strains were cultured by standard methods (Sherman, 1991), using rich (YPD) media or defined media, synthetic complete (SC), lacking the appropriate amino acids or nucleotides. Wild-type strain FY86 was obtained from Fred Winston (Harvard Medical School, Boston, MA). Genetic techniques, including matings, sporulations, and plasmid transformations with electroporation, were performed by standard methods (Rose *et al.*, 1989; Guthrie and Fink, 1991).

For temperature-shift experiments, cells cultured in liquid media at room temperature were shifted to a 37°C water bath, and incubation was continued as indicated in the figure legends. To prepare growth curves, single colonies of wild-type, mutant, or suppressed yeast cells were inoculated into 5 ml of SC-Leu and allowed to grow overnight at room temperature. Cell density was determined with a hemocytometer. Duplicate cultures of each strain were diluted to between 1 and 2 × 10⁶ cells/ml in SC-Leu and recounted. One

duplicate was incubated at 23°C and the other at 37°C. Duplicate samples were removed from each culture after various times up to 30 h, and the cell number was determined by counting.

Isolation of Suppressors and Identification of *RSS1*

To isolate high-copy suppressors of the *rat7-1* allele, we grew cells (LGY101) to an optical density (OD) of 1.4 (mid-log phase) and transformed them with electroporation by using a yeast genomic library present in the high-copy plasmid YEp13 (Nasmyth and Tatchell, 1980). Transformants were plated on SC-Leu plates and incubated at the restrictive temperature of 37°C. Colonies that appeared contained putative high-copy suppressors. To confirm that the suppression was due to a gene present on the library plasmid and not to a secondary mutation in the strain genome, we retrieved the plasmid from individual strains that grew at 37°C and tested it for its ability to restore growth at 37°C to *rat7-1* cells (LGY101). Plasmids were digested with various restriction endonucleases to identify those that contained overlapping DNA fragments. The majority of plasmids identified contained either *RAT7/NUP159*, fragments of *RAT7/NUP159*, or the region of chromosome IV containing the *RSS1* gene, the subject of this report.

RSS1 was cloned by retrieving the plasmid containing the library fragment with the suppressor gene from the *rat7-1* mutant strain. Both ends of the library fragment were sequenced with an ABI373 automated sequencer. These identified a region of yeast chromosome IV that had been sequenced as part of the yeast genome sequencing project and contained multiple open reading frames. The nucleotide sequence of this portion of chromosome IV was determined by an Applied Biosystems 373 (Foster City, CA) automated sequencer that used fluorescent dye terminators and cycle sequencing. The sequence of both DNA strands was determined. Results of one set of sequencing reactions were used to design primers to permit extension of the sequence.

Table 1. Yeast strains

Strain	Genotype	Comments
FY86	<i>MATα ura3-52 his3Δ200 leu2Δ1</i>	Wild-type; derived from S288C; (Winston <i>et al.</i> , 1995)
LGY101	<i>MATα ura3-52 his3Δ200 leu2Δ1 rat7-1^{ts}</i>	Segregant from 3rd backcross (Gorsch <i>et al.</i> , 1995)
VDPY102	<i>MATα ura3-52 his3Δ200 leu2Δ1 rat7-1^{ts} [pVDP2: LEU2 RSS1 2μ]</i>	pVDP2 isolated as a high-copy suppressor of <i>rat7-1</i>
VDPY107	<i>MATα ura3-52 his3Δ200 leu2Δ1 rat7-1^{ts} [pVDP7: LEU2 RSS1 2μ]</i>	pVDP7: <i>RSS1</i> ORF subcloned into YEpLac181
ACY1	<i>MATα/MATα ura3-52/ura3-52 leu2Δ1/leu2Δ1 his3Δ200/his3Δ200 trp1Δ63/TRP1</i>	provided by Dr. Anita Corbett, Harvard Medical School, Boston, MA
VDPY108	<i>MATα/MATα ura3-52/ura3-52 leu2Δ1/leu2Δ1 his3Δ200/his3Δ200 trp1Δ63/TRP1 RSS1/RSS1::HIS3</i>	heterozygous diploid <i>rss1</i> null strain
VDPY109	<i>MATα/MATα ura3-52/ura3-52 leu2Δ1/leu2Δ1 his3Δ200/his3Δ200 trp1Δ63/TRP1 RSS1/RSS1::HIS3 [pVDP9: URA3 RSS1 CEN]</i>	heterozygous diploid <i>rss1</i> null strain harboring <i>RSS1</i> plasmid
VDPY111	<i>MATα ura3-52 leu2Δ1 his3Δ200 trp1Δ63 RSS1::HIS3 [pVDP9: URA3 RSS1 CEN]</i>	haploid <i>rss1</i> null resulting from VDPY109 sporulation
VDPY112	<i>MATα ura3-52 leu2Δ1 his3Δ200 trp1Δ63 RSS1::HIS3 [pVDP12: LEU2 RSS1_{myc} CEN]</i>	haploid <i>rss1</i> null strain harboring <i>RSS1_{myc}</i> -containing plasmid
VDPY113	<i>MATα ura3-52 leu2Δ1 his3Δ200 trp1Δ63 RSS1::HIS3 [pVDP13: LEU2 RSS1_{myc} 2μ]</i>	haploid <i>rss1</i> null strain harboring <i>RSS1_{myc}</i> in a 2μ plasmid
VDPY114	<i>MATα ura3-52 leu2Δ1 his3Δ200 trp1Δ63 RSS1::HIS3 [pVDP14: LEU2 GAL::RSS1 CEN]</i>	haploid <i>rss1</i> null strain harboring <i>GAL1::RSS1</i> -containing plasmid
VDPY115	<i>MATα ura3-52 leu2Δ1 his3Δ200 trp1Δ63 RSS1::HIS3 [pVDP15: LEU2 GAL::RSS1_{myc} CEN]</i>	haploid <i>rss1</i> null strain harboring <i>GAL1::Rss1_{myc}</i> -containing plasmid
OLY101	<i>MATα his3Δ200 leu2Δ1 ura3-52 rat3-1/nup133-1</i>	Li <i>et al.</i> , 1995
CCY282	<i>MATα trp1Δ63 ura3-52 leu2Δ1 rat2-1/nup120-1</i>	Heath <i>et al.</i> , 1995
AGY401	<i>MATα ura3-52 leu2Δ1 trp1Δ63 rat9-1/nup85-1</i>	Goldstein <i>et al.</i> , 1996
AGY48	<i>MATα his3Δ200 leu2Δ1 ura3-52 nup145-10</i>	Dockendorff and Cole, unpublished data

Table 2. Plasmids

Plasmids	Markers	Comments
pVDP2	LEU2 2 μ Amp ^r	YEp13 containing the library fragment with <i>RSS1</i>
pVDP7	LEU2 2 μ Amp ^r	<i>RSS1</i> subcloned into YEpLac181
pVDP8	LEU2 CEN4 Amp ^r	<i>RSS1</i> subcloned into YCpLac111
pVDP9	URA3 CEN4 Amp ^r	<i>RSS1</i> subcloned into YCpLac33
pVDP12	LEU2 CEN4 Amp ^r	myc-tagged <i>RSS1</i> subcloned into YCpLac111
pVDP13	LEU2 2 μ Amp ^r	myc-tagged <i>RSS1</i> subcloned into YEpLac181
pVDP14	LEU2 CEN4 Amp ^r	<i>RSS1</i> ORF subcloned into YCpGAL1
pVDP15	LEU2 CEN4 Amp ^r	myc-tagged <i>RSS1</i> ORF subcloned into YCpGAL1

The ORF responsible for suppression of the *rat7-1* mutation was identified by deleting various ORFs contained in the library plasmid, transforming the derived plasmids back into *rat7-1* cells, and plating at 37°C. The *RSS1* ORF and flanking regulatory regions sufficient for suppression of the *rat7-1* mutation were subcloned into YepLac181 (Gietz and Sugino, 1988).

Disruption of *RSS1*

A polymerase chain reaction (PCR)-based gene deletion approach was used to delete *RSS1* (Baudin *et al.*, 1993). By PCR amplification, a cassette was generated that contained the yeast *HIS3* gene flanked at its ends by 45 nucleotides identical to sequences just upstream and downstream of the *RSS1* coding region. For both oligonucleotides used for PCR, the last 17 nucleotides are identical to sequences at the ends of the *HIS3* selectable gene. The oligo sequences are the following: for the 5' end, 5'-CGAAGAATGAGATTTGTTCGATGAGGTTTTCAATTCAGATACTGGCCTCCTCTAGTACTACTC-3'; and for the 3' end, 5'-GTGCATATATAAGTTCAGAAATTTCTAAGGAGACATTTCCGGAAAGCGCGCCTCGTTCAGAATG-3'. We used plasmid pBM2815 (obtained from P. Silver, Harvard Medical School, Boston, MA) containing the *HIS3* gene as a template in the PCR reaction. The PCR conditions were 30 cycles with denaturation at 94°C for 1.5 min, annealing at 50°C for 2.0 min, and extension at 72°C for 2.0 min. The PCR product was transformed into a wild-type diploid strain (ACY1), homozygous for *his3 Δ 200*. The flanking upstream and downstream sequences targeted the deletion construct to the *RSS1* locus such that the *RSS1* ORF was replaced with *HIS3* by homologous recombination. Recombinants were selected by plating the transformed cells on SC-His plates. Homologous recombination at this locus was verified by PCR and by Southern analysis.

To determine whether *RSS1* is essential for vegetative growth, we transformed the strain heterozygous for *RSS1* (VDPY108) with pVDP9, which contains WT *RSS1* in YCpLac33 (*ura*⁺). The transformants (VDPY109) were sporulated, the tetrads were dissected, and the four-spore tetrads were scored for auxotrophic markers and for the ability to grow on 5-FOA plates.

GAL1::RSS1 and *GAL1::RSS1_{myc}* Constructs

A *Pst*I-*Hind*III fragment containing the *RSS1* ORF was subcloned into the *Bam*HI-*Hind*III sites of the YCpGAL1 vector (provided by Anita Corbett, Harvard Medical School, Boston, MA). The resulting plasmid (pVDP14) was transformed into VDPY111 strain, and the

plasmid-borne wild-type copy of *RSS1* was eliminated by plating cells onto 5-FOA. To obtain the *GAL1::RSS1_{myc}* construct, a fragment of the *RSS1* ORF containing the "myc" epitope at its carboxy terminus was subcloned by similar procedures.

In Situ Hybridization and Immunofluorescence Assays

In situ hybridization assays for poly(A)⁺ RNA localization and indirect immunofluorescence (IF) techniques for protein localization have been described previously (Amberg *et al.*, 1992; Copeland and Snyder, 1993). Antibody against Rat7p/Nup159p raised in guinea pigs (Gorsch *et al.*, 1995) was used at 1:3000 dilution. FITC-conjugated goat anti-guinea pig immunoglobulin G (IgG; Vector Laboratories, Burlingame, CA) was used at 1:250 dilution. RL-1 monoclonal antibody (a gift from Larry Gerace, Scripps Research Institute, La Jolla, CA; Snow *et al.*, 1987) was used at a dilution of 1:200. FITC-conjugated goat anti-mouse IgM (Vector Laboratories) was used at a dilution of 1:600. Monoclonal antibody 2.3B, which recognizes nucleolar Nsr1p in yeast (a gift from M. Snyder, Yale University, New Haven, CT), was used at a dilution of 1:10. FITC-conjugated goat anti-mouse IgG (Vector Laboratories) was used at a dilution of 1:600.

For all fluorescence microscopy, images were obtained by using a cooled CCD (charge-coupled device) camera. Identical exposure conditions were used for all comparable images within each figure; that is, all fluorescein isothiocyanate (FITC) images within a single figure were obtained by using the same exposure conditions, as were all 4',6-diamidino-2-phenylindole (DAPI) images, although the exposure conditions for FITC images and for DAPI images were not the same. Composites were prepared with Adobe Photoshop without altering the images.

Analysis of Pre-rRNA Processing by Pulse Labeling

RNA was extracted by the method of Tollervey (Snow *et al.*, 1987), and the incorporation of [³H]-uridine into rRNA and its precursors was monitored as described previously (Heath *et al.*, 1995).

Epitope Tagging and Immunolocalization

Site-directed mutagenesis was used to create a unique restriction endonuclease site near the C terminus of the *RSS1* gene where the sequence encoding three copies of the epitope recognized by the 9E10 anti-myc monoclonal antibody was inserted in frame within the *RSS1* coding region. The triple myc tag was inserted into a *Bam*HI site created at amino acid 529 (total of 538 amino acids) by using a site-directed mutagenesis kit (Clontech Laboratories, Palo Alto, CA). The plasmid containing the myc-tagged *RSS1* (pVDP12 or pVDP13) was transformed into the strain VDPY111 carrying a disruption of *RSS1* and a plasmid containing a wild-type copy of *RSS1* (pVDP9). After selection on SC-Leu, the plasmid containing the wild-type *RSS1* gene was eliminated by plating onto 5-FOA. Cells carrying the myc-tagged *RSS1* allele (VDPY112, VDPY113) were subjected to indirect immunofluorescence. The primary antibody used was 9E10 mouse IgG monoclonal anti-myc from tissue culture hybridoma cells (a gift from Drs. J. Zhu and J.M. Bishop, University of California, San Francisco, CA) at a dilution of 1:1. The secondary antibody used was FITC-conjugated goat anti-mouse IgG (Vector Laboratories) at a dilution of 1:100.

To examine colocalization of Rss1p_{myc} and NPC antigens, we stained cells simultaneously with the RL-1 anti-nucleoporin antibody (1:200 dilution) and the 9E10 anti-myc monoclonal antibody (1:1 dilution). RL-1 is an IgM, and 9E10 is an IgG. We used FITC-conjugated goat anti-mouse IgG (1:100 dilution) to visualize the sites where Rss1p_{myc} was located and used Texas Red-conjugated goat anti-mouse IgM (1:600 dilution) to visualize where RL-1 antigens were located. When the FITC-conjugated secondary antibodies were left out, there was no signal from the Texas Red secondary

antibody in the FITC channel; similarly, when the Texas Red-conjugated secondary antibodies were left out, there was no signal from the FITC-conjugated secondary antibody in the Texas Red channel.

Western Analysis

Cells were grown to a total OD₆₀₀ of 0.75. Cells were pelleted by centrifugation at 2500 rpm for 2.5 min and washed once with water. Acid-washed glass beads (200 mg) and 200 μ l of hot sample buffer (62.5 mM Tris-Cl, pH 6.8, 2% SDS, 10% glycerol, 8 M urea, 0.72 M 2-mercaptoethanol, and 0.05% bromophenol blue) were added to the cell pellets. After brief vortexing, cells were transferred to a 100°C water bath for 3 min. Cells were then lysed as follows: 10 s of vortexing and 50 s of incubation in a 100°C water bath, repeated five times during 5 min. The supernatant was then transferred to a clean Eppendorf tube, and equal volumes of cell lysate were loaded onto a 10% SDS-polyacrylamide gel. The gel was run at 200 V for ~50 min. Proteins in the gel were transferred to a polyvinylidene difluoride (PVDF) membrane by electroblotting overnight at 100 mA in a cold room. The membrane was briefly washed with a 1 \times PBS, 0.1% Tween 20 solution (solution A) and then blocked for 1 h with a 1 \times PBS, 0.1% Tween 20, 5% nonfat milk solution (solution B). The membrane was then incubated with 9E10 anti-myc monoclonal antibody at a 1:10 dilution in solution B for 2 h. Four washes of 10 min each were done with solution A. The membrane was then incubated with anti-mouse antibody coupled to the enzyme (Amersham, Arlington Heights, IL) diluted 1:3000 in solution B for 1 h. Washes were performed as before (see above). Signal was developed by treating the membrane with the enhanced chemiluminescence (ECL) kit (Amersham). As a control for loading, membranes were incubated with polyclonal rabbit anti-Sec13p antibody (kindly provided by Dr. Charles Barlowe, Dartmouth Medical School, Hanover, NH) at a 1:2000 dilution and anti-rabbit antibody coupled to horseradish peroxidase (Amersham) at a 1:10,000 dilution.

Electron Microscopy

S. cerevisiae were examined by electron microscopy with the following previously described protocols: Byers and Goetsch (1975), Wright and Rine (1989), and Goldstein *et al.* (1996). Sections were cut on a Sorvall MT5000 (RMC, Tucson, AZ) ultramicrotome with a section thickness of 90 nm and examined on a JEOL 100CX (Peabody, MA) electron microscope at 80 kV.

RESULTS

Identification of RSS1 in a Screen for High-Copy Extragenic Suppressors of the *rat7-1 ts* Allele

To identify proteins that might interact with Rat7p/Nup159p, we performed a high-copy extragenic suppressor screen of the *rat7-1 ts* allele. The *rat7-1* strain (LGY101) was grown to mid-log phase and transformed by electroporation with a yeast genomic library present in a 2 μ -based, high-copy vector. The transformants were plated at 37°C to select for those that acquired the ability to grow at the nonpermissive temperature because of the presence of a library plasmid. More than 30,000 colonies were screened and 38 putative suppressors isolated. The results are summarized in Table 3. We isolated plasmids containing the complete *RAT7/NUP159* gene several times, as well as DNA fragments encoding the C-terminal portion of the Rat7p/Nup159p. The fact that the C-terminal end of Rat7p/Nup159p can suppress the *rat7-1 ts* allele

Table 3. Suppressor screening

High-copy suppressors	Number of times isolated
Extragenic	
Suppressor 9/RSS1 ^a	4
Suppressor 3	1
Suppressor 4	1
Suppressor 8	1
Intragenic	
RAT7/NUP159	22
C-terminal domain of RAT7/NUP159	6
Revertants	3
Total	38

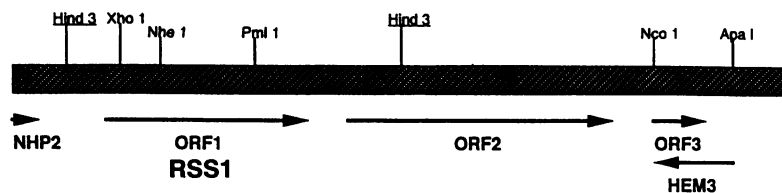
^a Rat Seven Suppressor.

suggests that this domain probably plays a critical role in the function of Rat7p/Nup159p, and further studies of this possibility are in progress. In addition to these intragenic suppressors, we isolated a number of extragenic suppressors. One of these was independently identified four times, and we call this gene *RSS1* (Rat Seven Suppressor 1). Because of the frequency with which *RSS1* was isolated, it was selected for further study.

To identify the *RSS1* gene, the plasmid containing this extragenic suppressor was retrieved from the *rat7-1* strain, and DNA sequence was obtained from both ends of the library fragment. This sequencing data positioned *RSS1* on chromosome IV between *NHP2* and *HEM3*. The suppressing plasmid contained three new ORFs in addition to the fragments of *NHP2* and *HEM3* (Figure 1A). To determine which of the ORFs corresponded to *RSS1*, we deleted each putative ORF individually, the religated library vector was transformed into *rat7-1* cells, and cells were plated at 37°C. When ORF1 was deleted, the growth defect at 37°C of *rat7-1* cells could not be suppressed, indicating that this ORF was likely *RSS1*. To confirm, we subcloned ORF1 and flanking regulatory signals into YepLac181 (to produce pVDP7), and we found them to suppress the growth defect of *rat7-1* cells at 37°C.

RSS1 encodes a novel protein of 538 amino acids with a predicted molecular weight of 62 kDa and a pI of 9.03. The sequence of this protein is shown in Figure 1B. An extended segment of Rss1p (amino acids 124–255) is predicted (Lupas *et al.*, 1991) to have a very high potential ($p > 99.9\%$) to form a coiled-coil structure (Figure 1C). No other obvious structural features or motifs were found. Rss1p shows no homology with other proteins outside of its potential coiled-coil region.

To determine whether *RSS1* is an essential gene, we replaced the *RSS1* coding region with the *HIS3* gene. Haploid cells containing the disrupted copy of *RSS1*

A**B**

```

1 MRFVFDEVFN SDTDSPEFEE TCSTTSSTSS QCPTPEPSA IKLPSFTKVG TKKLVNESV
61 ILDPALLENAL RDLNLQSKLI PINEPIVAAS SIIVPHSTNM PLPRASHSSL LDNAKNSNAT
121 APLLEAIEES FQRKMQNLVL ANQKEIQSIR ENKRRVEEQR KRKEEEERKR KEAEEKAKRE
181 QELLRQKKDE EERKRKEAEA KLAQQQEEE RKKIEEQNEK ERQLKKEHEA KLLQQKDKLG
241 KAVTNFDKIS KMFWHYKDKI AQIKQDIVLP IKKADVNRN LLSRHKRIN PKFGQLTNSN
301 QQLFKIQNEL TQLINDTKGD SLAYHWILNF IAKAVVHQAE TEVRVKPESA LPLGKLTLYL
361 LVQFPELQEL FMARLVKKCP FVIGFTCEID TEKGRQNMGW KRNNENKWED NTSYDERMGG
421 ILSLFAIITR LQLPQEFITT TSHFPPIALS WHILARICNT PLNLITNTHF VILGSWWDAA
481 AVQFLQAYGN QASKLLILIG EELTSRMAEK KYVGAARLRI LLEAWQNNM ESFPEMSP

```

C

Coiled-coil probability of Rss1p

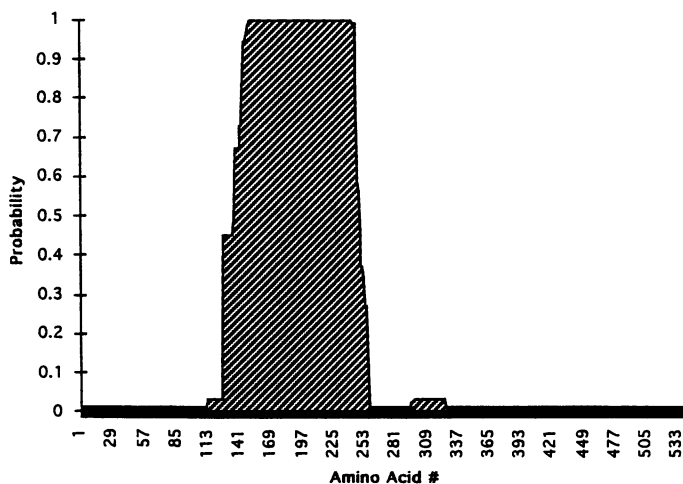


Figure 1. The *S. cerevisiae* *RSS1* gene. (A) Schematic representation of the region of yeast chromosome IV in which *RSS1* is located. Important restriction endonuclease digestion sites are shown. The arrows show the putative ORFs in this region. The two *Hind*III sites indicated were used to subclone *RSS1*. (B) Predicted amino acid sequence of *Rss1p*, which contains 538 amino acids. (C) Coiled-coil probability for *Rss1p*; the PEPCOIL program was used to search *Rss1p* for potential coiled-coil regions (Lupas *et al.*, 1991).

were not able to grow in the absence of a plasmid containing the *RSS1* gene, indicating that *RSS1* is essential for growth. We also transformed pVDP7 (the Yeplac181 vector containing *RSS1*) into a strain containing a disruption of *RAT7/NUP159* and containing the wild-type *RAT7/NUP159* gene on a *URA3/CEN* plasmid. These cells were unable to grow on 5-FOA, indicating that overexpression of *RSS1* cannot bypass the need for *Rat7p/Nup159p*. When the *RSS1* gene was cloned into a *CEN* plasmid, it was no longer able to suppress the *rat7-1* growth defect at 37°C, indicating that overexpression of *RSS1* is required for suppression.

To determine whether suppression of *rat7-1* by high-copy *RSS1* was specific for the *rat7-1* mutant allele, we introduced pVDP7 into strains carrying the *rat2-1/nup120-1*, *rat3-1/nup133-1*, *rat9-1/nup85-1*, and *nup145-10* ts mutant alleles. The transformants were plated both at 23 and 37°C. At 23°C, the growth of none of the strains was affected by the *RSS1* suppressor. However, no growth was detected in any of the strains at the restrictive temperature in the presence of high-copy *RSS1*. These data indicate that *RSS1* is not a general suppressor of ts alleles of yeast nucleoporins.

Partial Suppression of *rat7-1* Defects by High-Copy *RSS1*

rat7-1 cells rapidly stop growing when shifted to the nonpermissive temperature of 37°C (Gorsch *et al.*, 1995). To determine how well *RSS1* in high copy suppressed the growth defect of *rat7-1* cells at 37°C, we monitored the growth rates of wild-type and *rat7-1* cells in the presence and absence of *RSS1* (Figure 2). At the permissive temperature (23°C), the growth behavior of the *rat7-1* was the same in the presence or absence of high-copy *RSS1*, but cells did not multiply as rapidly as wild-type cells. At 37°C, the presence of high-copy *RSS1* permitted *rat7-1* cells to grow at 37°C at a rate essentially identical to that of *rat7-1* cells at 23°C. However, this growth rate was still below that of wild-type cells (FY86). Thus, high-copy *RSS1* partially suppressed the growth defect of *rat7-1* cells at 37°C, and its overexpression had no deleterious effect on the growth of *rat7-1* or wild-type cells at 23°C.

rat7-1 cells accumulate poly(A)⁺ RNA in their nuclei rapidly after a shift to the restrictive temperature. After 15 min at 37°C, 100% of the cells show dramatically enhanced nuclear accumulation of poly(A)⁺ RNA (Gorsch *et al.*, 1995). We examined the effect of high-copy *RSS1* on mRNA export in *rat7-1* cells by using fluorescence in situ hybridization. Figure 3 shows the subcellular location of poly(A)⁺ RNA in wild-type cells, *rat7-1* cells, and *rat7-1* cells in the presence of high-copy *RSS1*, both at the permissive and restrictive temperatures. In all three strains grown at 23°C, poly(A)⁺ RNA was distributed throughout the cell, although some nuclear accumulation of poly(A)⁺ RNA was seen in *rat7-1* cells (Figure 3E), even in the presence of high-copy *RSS1* (Figure 3I). After a 2-h shift to 37°C, nuclear accumulation of poly(A)⁺ RNA was seen in 100% of *rat7-1* cells with almost no cytoplasmic signal (Figure 3G). Poly(A)⁺ RNA was found often in a pattern of multiple punc-

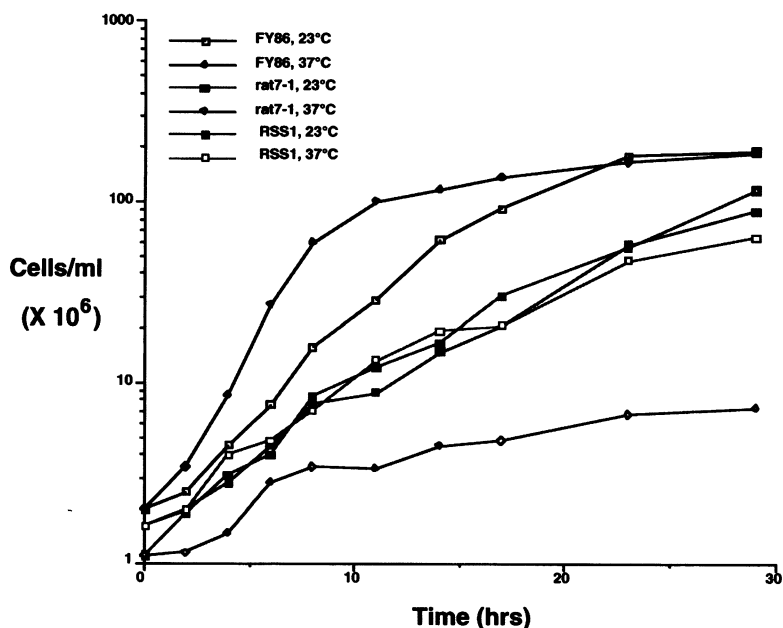
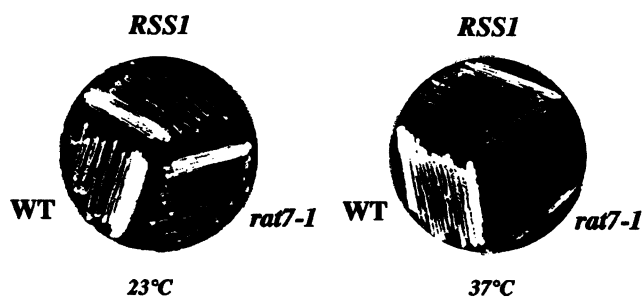


Figure 2. Comparison of the growth characteristics of strains FY86 (WT), LGY101 (*rat7-1*), and VDPY (*rat7-1* and containing *RSS1* on a 2 μ plasmid) at 23 and 37°C. Cells were allowed to reach stationary phase and diluted; then growth was monitored at both 23 and 37°C. Duplicate samples were taken after 2, 3, or 6 h of growth, and cells were counted with a hemacytometer. Each point is an average of cell counts from duplicate samples. Strains were also grown on SC-Leu plates for 4 d at 23 or 37°C.



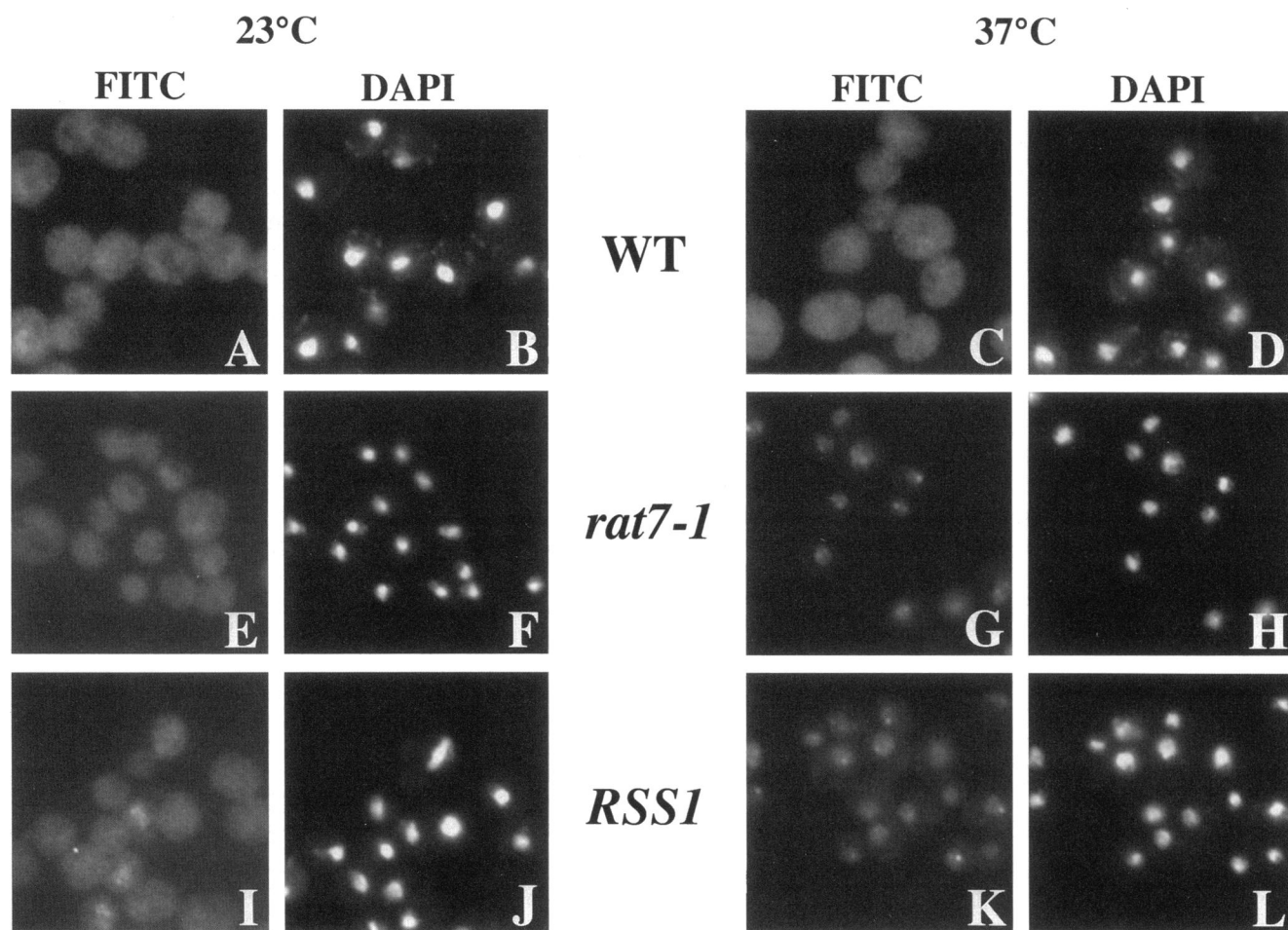


Figure 3. High-copy *RSS1* partially suppresses the mRNA export defect of *rat7-1* cells. (A–D) WT (FY86); (E–H) *rat7-1* cells; (I–L) *RSS1* (*rat7-1* cells transformed with pVDP7). Cells were grown to mid-log phase at 23°C and then either left at 23°C (A, B, E, F, I, and J) or shifted to 37°C for 2 h (C, D, G, H, K, and L). Cells were then fixed with formaldehyde and subjected to in situ hybridization by using a digoxigenin-tagged oligo (dT50) probe to detect poly(A)⁺ RNA. Hybridizing probe was visualized by FITC-conjugated anti-digoxigenin antibody (A, C, E, G, I, and K). The same fields of cells were also stained with DAPI (B, D, F, H, J, and L). Images were taken by using a cooled CCD camera. (A) WT, 23°C, FITC; (B) WT, 23°C, DAPI; (C) WT, 37°C, FITC; (D) WT, 37°C, DAPI; (E) *rat7-1*, 23°C, FITC; (F) *rat7-1*, 23°C, DAPI; (G) *rat7-1*, 37°C, FITC; (H) *rat7-1*, 37°C, DAPI; (I) high-copy *RSS1*, 23°C, FITC; (J) high-copy *RSS1*, 23°C, DAPI; (K) high-copy *RSS1*, 37°C, FITC; (L) high-copy *RSS1*, 37°C, DAPI.

tate spots, which colocalize with nucleolar antigens (Del Priore and Cole, unpublished results). When *rat7-1* cells containing high-copy *RSS1* were shifted to 37°C for 2 h, most of the poly(A)⁺ RNA signal was present in the nucleus, but there was also a clear cytoplasmic signal that was not present in *rat7-1* cells lacking high-copy *RSS1* (Figure 3, compare K with G). However, this cytoplasmic signal was much weaker than the cytoplasmic signal seen in wild-type cells shifted to 37°C (Figure 3C). No changes in signal intensities were seen when these cultures were shifted to 37°C for 4 h (Del Priore and Cole, unpublished results). We conclude that high-copy *RSS1* partially suppressed the block to mRNA export caused by the *rat7-1* mutation.

Fragmentation of the nucleolus after a shift to 37°C has been observed at the nonpermissive temperature in several yeast strains defective for mRNA export (Kadowaki *et al.*, 1994, 1995; Heath *et al.*, 1995; Goldstein *et al.*, 1996), including strains carrying the *rat7-1* allele (Heath *et al.*, 1995). To examine nucleolar fragmentation in *rat7-1* cells grown at 23°C or shifted to 37°C for 2 h, we performed indirect immunofluorescence analysis with a monoclonal antibody against the nucleolar protein, Nsr1p (monoclonal antibody 2.3B). The results are shown in Figure 4. When grown at the permissive temperature, *rat7-1* cells show a distribution of the nucleolar antigen that is the same as wild type (Figure 4, compare A and E). The signal is present in a cres-

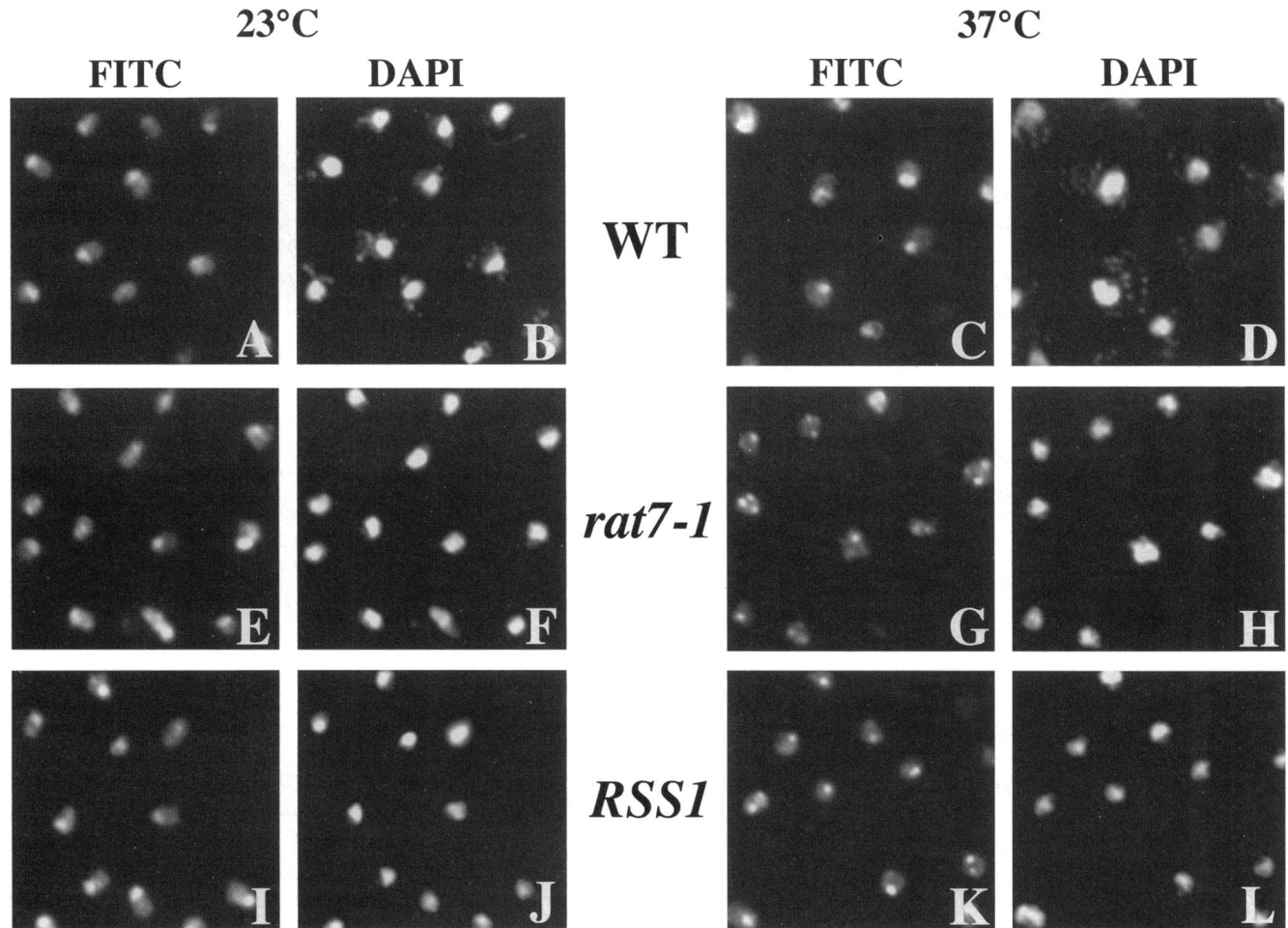


Figure 4. Indirect immunofluorescence with an anti-fibrillar antibody to test for nucleolar fragmentation. (A–D) WT (FY86); (E–H) *rat7-1*; (I–L) high-copy *RSS1* (*rat7-1* cells transformed with pVDP7). Cells were grown to mid-log phase at 23°C and then either maintained at that temperature (A, B, E, F, I, and J) or shifted to 37°C for 2 h (C, D, G, H, K, and L). Fixation and immunofluorescence techniques were performed by following the protocol described in MATERIALS AND METHODS. The DAPI images are of the same fields of cells as the FITC images to their left. (A) WT, 23°C, FITC; (B) WT, 23°C, DAPI; (C) WT, 37°C, FITC; (D) WT, 37°C, DAPI; (E) *rat7-1*, 23°C, FITC; (F) *rat7-1*, 23°C, DAPI; (G) *rat7-1*, 37°C, FITC; (H) *rat7-1*, 37°C, DAPI; (I) high-copy *RSS1*, 23°C, FITC; (J) high-copy *RSS1*, 23°C, DAPI; (K) high-copy *RSS1*, 37°C, FITC; (L) high-copy *RSS1*, 37°C, DAPI.

cent-shaped pattern, and the DAPI signal, which represents DNA staining, seems to be excluded from the location where the intensity of the nucleolar signal reaches its maximum. When shifted to 37°C, wild-type cells displayed the same distribution of the nucleolar antigen that was seen at 23°C (Figure 4C). In contrast, after a 2-h shift to 37°C, there was a dramatic fragmentation of the nucleoli in *rat7-1* cells, in agreement with our previous findings (Heath *et al.*, 1995). In almost all cells, two to three nucleolar fragments can be seen (Figure 4G). Fragmentation was detected as soon as 20 min after shifting to the nonpermissive temperature (Gorsch and Cole, unpublished results).

When grown at the permissive temperature, the *rat7-1* cells containing high-copy *RSS1* displayed the

same pattern for nucleolar antigen distribution as wild-type and *rat7-1* cells (Figure 4, compare I with A and E). After a 2-h shift to the nonpermissive temperature of 37°C, less dramatic nucleolar fragmentation was seen in the presence of high-copy *RSS1* than in similarly treated *rat7-1* cells (Figure 4, compare K with G). Only a few cells showed fragmentation of the nucleolus, although few cells show the crescent-shaped morphology seen in wild-type cells. Thus, when *RSS1* was present in high-copy in *rat7-1* cells, the nucleolar fragmentation phenotype observed in the absence of *RSS1* was partially suppressed.

In temperature-sensitive yeast strains in which nucleolar disruption is seen after a shift to the nonpermissive temperature, defects in rRNA synthesis

and processing have also been reported (Traglia *et al.*, 1989; Aebi *et al.*, 1990). The fact that the *rat7-1* strain showed a severe nucleolar disruption phenotype when shifted to the nonpermissive temperature prompted us to determine whether it also showed defects in rRNA processing. We performed a [³H]-uridine incorporation assay in wild-type and *rat7-1* cells at both the permissive and nonpermissive temperatures. When *rat7-1* cells were shifted to 37°C, the incorporation of [³H]-uridine into precipitable counts decreased to 20% of the level of incorporation seen at 23°C within 15 min of the shift to 37°C and to 10% after a 30-min shift. The labeled rRNA produced was analyzed by electrophoresis and fluorography (Figure 5). The autoradiograph shows that there was no significant difference in rRNA processing between wild-type and *rat7-1* cells when both were grown at the permissive temperature (compare Figure 5, lanes 1 and 3). In contrast, after 1 h at 37°C, *rat7-1* cells accumulated the 35S precursor, which is the primary transcript of yeast rDNA genes, and an aberrant 23S RNA (Figure 5, lane 4). Accumulation of 35S and 23S rRNAs was also seen in the control strain carrying the *rna1-1* allele when it was shifted to 37°C for 40 min (Figure 5, lane 10), as has been reported previously (Traglia *et al.*, 1989). These defects could be seen as soon as 15 min after the temperature shift of *rat7-1* cells (Del Priore and Cole, unpublished results) and were more severe 2 h after the shift (Figure 5, lane 5).

To determine whether the presence of high-copy *RSS1* in *rat7-1* cells had any effect on the level of rRNA synthesis and the fidelity of rRNA processing when this strain was shifted to 37°C, we measured the incorporation of [³H]-uridine into precipitable counts. After a 1-h shift to 37°C, incorporation in the presence of high-copy *RSS1* was 20% of the level of incorporation seen at 23°C and subsequently increased to 30% of the 23°C incorporation after 2 h at 37°C. We then analyzed the labeled rRNA by electrophoresis. The data show that, in the presence of high-copy *RSS1*, there was a partial suppression of the rRNA processing defects seen in *rat7-1* cells at the restrictive temperature (Figure 5, compare lanes 7 and 8 with lanes 4 and 5). Accumulation of 35S rRNA was still detected but to a lesser degree than in *rat7-1* cells, and there was no significant accumulation of 23S rRNA. Thus, in *rat7-1* cells shifted to 37°C, there were defects in the levels of rRNA synthesis and in the kinetics and fidelity of processing of the 35S rRNA precursor. In the presence of high-copy *RSS1*, we observed partial suppression of the defects in the levels and kinetics of rRNA processing and no longer saw defects in the fidelity of processing.

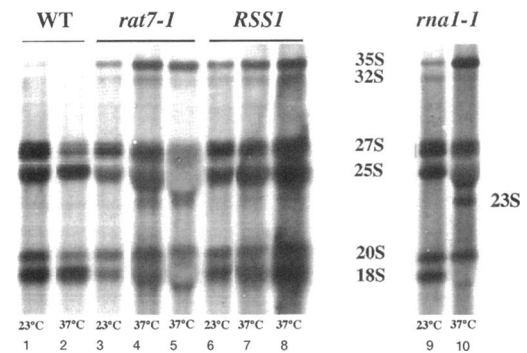


Figure 5. Analysis of rRNA processing. Cells were labeled with [³H]-uridine, and total RNA was isolated from WT (FY86), *rat7-1*, and high-copy *RSS1* (*rat7-1* transformed with pVDP7) cells grown either at 23°C or shifted to 37°C for 1 or 2 h. Labeled RNA was then analyzed by electrophoresis of approximately equal numbers of counts of labeled RNA in a 1.2% agarose-formaldehyde gel. As a control for rRNA processing defects, a strain carrying the *rna1-1* allele was included. (1) WT grown at 23°C; (2) WT grown at 37°C for 2 h; (3) *rat7-1* grown at 23°C; (4) *rat7-1* grown at 37°C for 1 h; (5) *rat7-1* grown at 37°C for 2 h; (6) high-copy *RSS1* grown at 23°C; (7) high-copy *RSS1* grown at 37°C for 1 h; (8) high-copy *RSS1* grown at 37°C for 2 h; (9) *rna1-1* grown at 23°C; (10) *rna1-1* grown at 37°C for 40 min. Asterisk indicates a 23S intermediate product often seen in strains with rRNA processing defects.

***Rat7p* Is Lost from NPCs at 37°C both in the Presence and Absence of High-Copy *RSS1*, but NPC Clustering Is Partially Maintained by *Rss1p* Overexpression**

When *rat7-1* cells are shifted to the nonpermissive temperature, the mutant *Rat7p* is rapidly lost from NPCs, as determined by immunofluorescence with an anti-*Rat7p* antibody (Gorsch *et al.*, 1995). To see whether overexpression of *Rss1p* was sufficient to maintain *Rat7p* at the nuclear rim, we examined the location of *Rat7p*/Nup159p by indirect immunofluorescence in wild-type cells and in *rat7-1* cells either lacking or containing high-copy *RSS1*. The results are shown in Figure 6. At 23°C, wild-type cells showed a punctuate staining pattern surrounding the nucleus (Figure 6A), which was localized by staining with DAPI (Figure 6B). As reported previously (Gorsch *et al.*, 1995), NPCs were clustered in *rat7-1* cells grown at 23°C (Figure 6F). An identical pattern of clustered NPCs was seen at 23°C in *rat7-1* cells containing high-copy *RSS1* (Figure 6K).

When cells were shifted to 37°C for 2 h, the anti-*Rat7p*/Nup159p antibody continued to stain wild-type cells with the same punctate rim staining pattern seen in cells grown at 23°C (Figure 6C). In contrast, no signal for *Rat7p*/Nup159p was detectable in *rat7-1* cells, either in the absence (Figure 6H) or presence (Figure 6M) of high-copy *RSS1*. Thus, the presence of high-copy *RSS1* was unable to prevent the loss from NPCs of mutant *Rat7p*/Nup159p when mutant cells were shifted to 37°C.

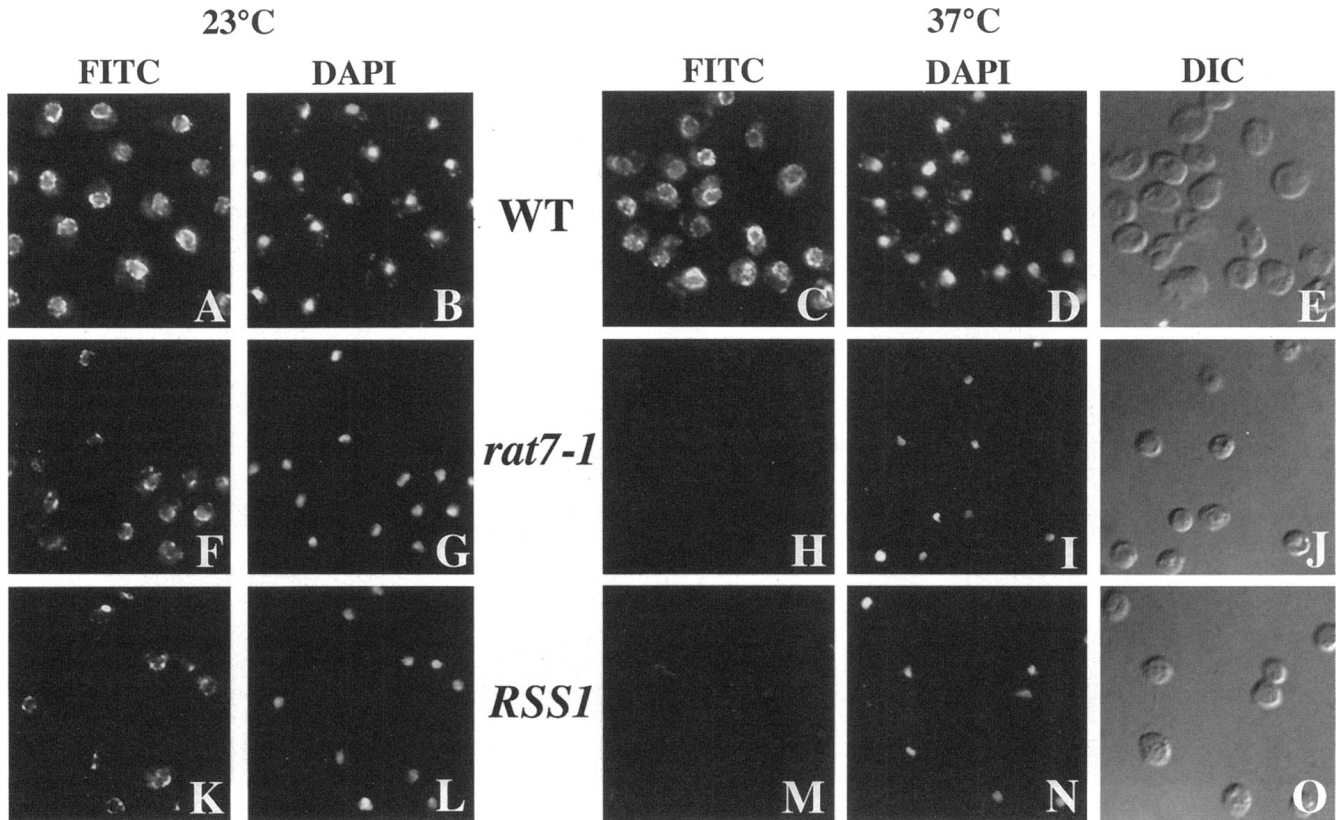


Figure 6. Indirect immunofluorescence with anti-Rat7p antibody. (A–E) WT (FY86); (F–J) *rat7-1*; (K–O) *RSS1* (*rat7-1* cells transformed with pVDP7). Cells were grown to mid-log phase at 23°C and then either maintained at that temperature (A, B, F, G, K, and L) or shifted to 37°C for 2 h (C–E, H–J, and M–O). Cells were then fixed and processed for indirect immunofluorescence with a polyclonal anti-Rat7p antibody, as described in MATERIALS AND METHODS. The DAPI and DIC images are of the same fields of cells as the FITC images to their left. (A) WT, 23°C, FITC; (B) WT, 23°C, DAPI; (C) WT, 37°C, FITC; (D) WT, 37°C, DAPI; (E) WT, 37°C, DIC; (F) *rat7-1*, 23°C, FITC; (G) *rat7-1*, 23°C, DAPI; (H) *rat7-1*, 37°C, FITC; (I) *rat7-1*, 37°C, DAPI; (J) *rat7-1*, 37°C, DIC; (K) high-copy *RSS1*, 23°C, FITC; (L) high-copy *RSS1*, 23°C, DAPI; (M) high-copy *RSS1*, 37°C, FITC; (N) high-copy *RSS1*, 37°C, DAPI; (O) high-copy *RSS1*, 37°C, DIC.

Clustering of NPCs is a common phenotype seen in yeast cells carrying mutant alleles of several different nucleoporins (Wente *et al.*, 1992; Wente and Blobel, 1993, 1994; Bogerd *et al.*, 1994; Doye *et al.*, 1994; Aitchison *et al.*, 1995; Gorsch *et al.*, 1995; Heath *et al.*, 1995; Li *et al.*, 1995; Pemberton *et al.*, 1995; Goldstein *et al.*, 1996). The *rat7-1* strain has a novel NPC clustering phenotype in that pores become considerably less clustered after a shift to 37°C (Gorsch *et al.*, 1995). This altered distribution of NPCs in *rat7-1* cells occurs rapidly, within 1 h of a shift to 37°C. To determine how high-copy *RSS1* affected this phenotype, we performed indirect immunofluorescence with the RL-1 monoclonal antibody, which recognizes NPC antigens in both metazoan and yeast cells (Snow *et al.*, 1987; Copeland and Snyder, 1993). At 23°C in wild-type cells and in *rat7-1* cells in the presence or absence of high-copy *RSS1*, the pattern of staining with the RL-1 antibody was the same as that seen with the anti-Rat7p antiserum (compare Figure 6, A, F, and K, with

Figure 7, A, F, and K, respectively). When shifted to 37°C for 2 h, a high percentage of *rat7-1* cells showed a redistribution of NPC antigens to a pattern that was very similar to the wild-type distribution (Figure 7, compare H with C), in agreement with observations reported previously (Gorsch *et al.*, 1995). In contrast, in the presence of high-copy *RSS1*, NPCs in *rat7-1* cells showed a tendency to retain their clustered distribution (Figure 7M).

We also examined *rat7-1* cells in the presence or absence of high-copy *RSS1* by thin-section electron microscopy. In different cells, NPCs were seen to be evenly distributed, grouped, or clustered. We considered NPCs to be clustered when all or almost all of the NPCs in a thin section were clustered together, forming a single “grape-like” structure. Pores were considered to be grouped when multiple NPCs were adjacent in the plane of the nuclear envelope. Often, multiple groups were seen in a single thin section, and additional isolated NPCs were also present. Cluster-

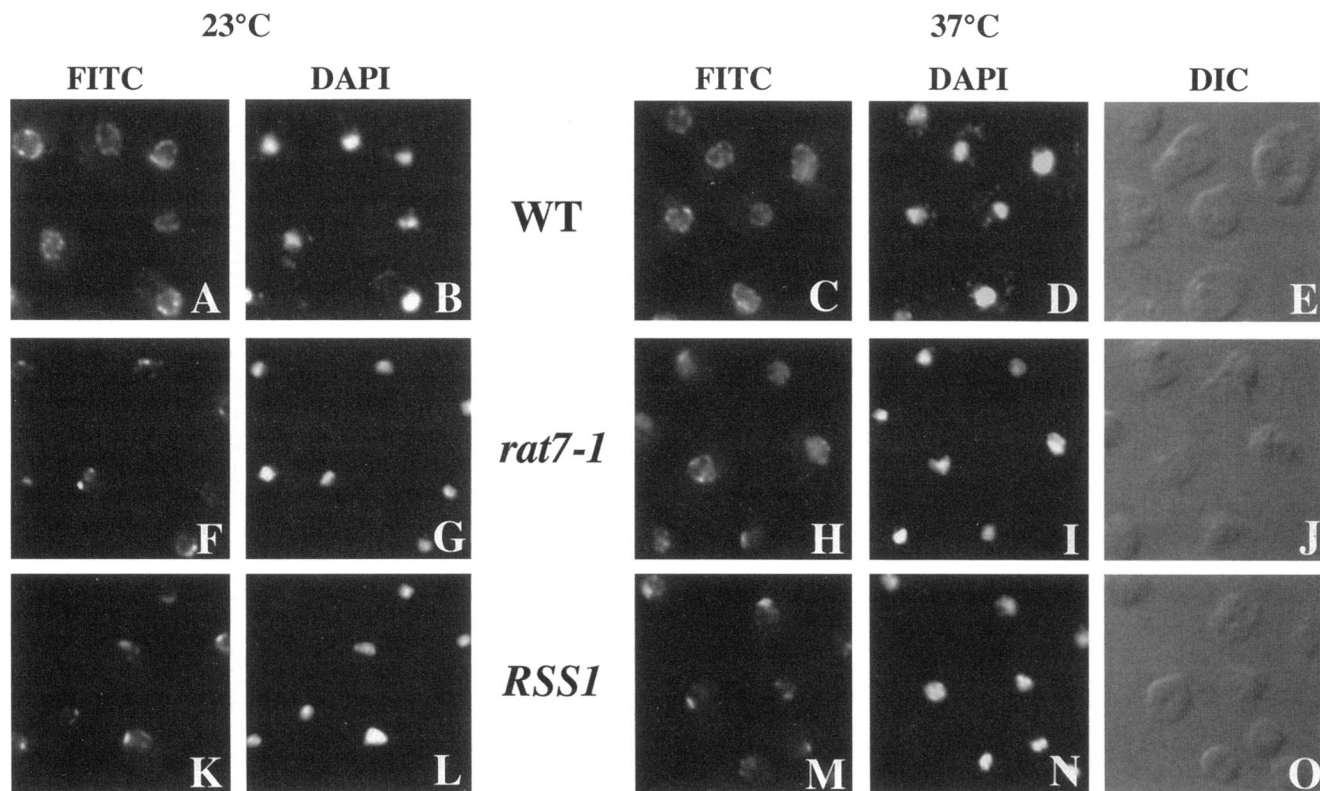


Figure 7. Indirect immunofluorescence to examine the distribution of NPCs. (A–E) WT (FY86); (F–J) *rat7-1*; (K–O) high-copy *RSS1* (*rat7-1* cells transformed with pVDP7). Cells were grown to log phase at the permissive temperature and then either maintained at 23°C (A, B, F, G, K, and L) or shifted to the nonpermissive temperature of 37°C (C–E, H–J, and M–O). After fixation and processing for indirect immunofluorescence, cells were incubated with the RL-1 monoclonal antibody, which recognizes NPC proteins from many organisms, including *S. cerevisiae*. The DAPI and DIC images are of the same fields of cells as the FITC images to their left. (A) WT, 23°C, FITC; (B) WT, 23°C, DAPI; (C) WT, 37°C, FITC; (D) WT, 37°C, DAPI; (E) WT, 37°C, DIC; (F) *rat7-1*, 23°C, FITC; (G) *rat7-1*, 23°C, DAPI; (H) *rat7-1*, 37°C, FITC; (I) *rat7-1*, 37°C, DAPI; (J) *rat7-1*, 37°C, DIC; (K) high-copy *RSS1*, 23°C, FITC; (L) high-copy *RSS1*, 23°C, DAPI; (M) high-copy *RSS1*, 37°C, FITC; (N) high-copy *RSS1*, 37°C, DAPI; (O) high-copy *RSS1*, 37°C, DIC.

ing is a more extreme distribution pattern than grouping. We examined thin sections from 50 separate cells of each strain, and the data are summarized in Figure 8. Nuclei showing these different phenotypes are shown in Figure 9. Almost 80% of the thin sections of wild-type cells examined showed pores that were evenly distributed, whereas small groups of NPCs were seen in ~20% of the sections, and clusters were not observed. Figure 9, A and B, shows wild-type nuclei with NPCs that are either evenly distributed around the nucleus (A) or grouped (B). In *rat7-1* cells grown at 23°C, NPCs were either clustered or grouped in >80% of thin sections examined; grouping was more common than clustering. Figure 9, C and D, shows the nuclei of representative *rat7-1* cells grown at 23°C, with NPCs either clustered (C) or grouped (D). NPCs were substantially less clustered or grouped in *rat7-1* cells shifted to 37°C, with NPCs distributed evenly in 66% of the sections and with NPCs either grouped or clustered in 34%. Figure 9, E and F, shows *rat7-1* cells grown at 37°C, with NPCs

either distributed around the nucleus (E) or grouped (F). When *RSS1* was overexpressed in *rat7-1* cells grown at 23°C, there was little change in the NPC distribution patterns from those observed for *rat7-1* cells, with clustering or grouping observed in >70% of the cells. Figure 9, G and H, shows sections of *rat7-1* cells overexpressing *Rss1p* and grown at 23°C, with NPCs either clustered (G) or grouped (H). Although indirect immunofluorescence suggested little change in NPC distribution when these cells were shifted to 37°C, thin-section electron microscopy revealed a modest increase in the fraction of thin sections showing evenly distributed NPCs and a slight decrease in the fraction of sections showing clustered or grouped NPCs. Figure 9, I and J, shows nuclei from *rat7-1* cells overexpressing *RSS1* and shifted to 37°C, in which pores are either grouped (I) or more evenly distributed (J). The data indicate that NPCs remained more clustered or grouped in *rat7-1* cells shifted to 37°C when *RSS1* was overexpressed than in the absence of *RSS1* overexpression. This suggests that retention of

clustering and grouping may be important for partial suppression of the mRNA export defect in *rat7-1* cells by *RSS1*.

Immunolocalization of *Rss1p*

To determine the subcellular location of *Rss1p*, we tagged the protein with a triple "myc" epitope. The epitope was introduced at the C-terminal end of the protein (aa 529), where a *Bam*HI site was created by site-directed mutagenesis. The myc-tagged *RSS1* gene was able to complement fully an *RSS1* null strain when present on either low-copy (*CEN*) or high-copy (2μ) plasmids; however, it was unable to suppress the *rat7-1* mutation. Indirect immunofluorescence was performed with the 9E10 anti-myc antibody. When observed with conventional fluorescence microscopy, the cells showed a strong cytoplasmic signal and a weak rim staining around the nucleus (our unpublished results). Because the intense cytoplasmic signal seemed to be partially masking the nuclear rim pattern, samples were examined by confocal fluorescence microscopy, which showed more clearly that *Rss1p* is located both within the cytoplasm and at the nuclear rim (Figure 10). That portion of *Rss1p_{myc}* located at the nuclear rim colocalized with nucleoporins recognized by the RL-1 monoclonal antibody (Figure 10A) and with Rat7p/Nup159p (Del Priore and Cole, unpublished results). The tagged protein was also readily detected in the cytoplasm of yeast cells, and it was primarily this cytoplasmic signal that increased when the protein was overexpressed by placing the gene encoding *Rss1p_{myc}* in a high-copy (2μ) vector (Figure 10, compare A and B). As a control, indirect immunofluorescence was also performed to localize plasmid-borne myc-tagged nucleoporins, and no cytoplasmic signal was observed for either Rat7p/Nup159p_{myc} or Rat2p/Nup120p_{myc} (our unpublished results). We

conclude that *Rss1p* is located both at nuclear pores and in the cytoplasm.

Figure 10C shows a Western blot in which identical amounts of protein were loaded in each lane and the 9E10 anti-myc monoclonal antibody was used to detect *Rss1p_{myc}*, which migrated with an apparent molecular weight of ~66 kDa, very close to the expected position for this tagged protein. Comparison of lanes 2 and 3 indicate that *Rss1p_{myc}* was expressed at a level approximately eightfold higher when expressed from a high-copy plasmid (Figure 10C, lane 3) than when expressed from a *CEN* plasmid (Figure 10C, lane 2), consistent with the stronger fluorescent signal seen in Figure 10B in comparison with 10A. The 9E10 antibody also detected a band in wild-type cells (Figure 10C, lane 1) that migrated very closely to the position of *Rss1p_{myc}*. However, no immunofluorescent signal was detected in wild-type cells with this antibody (Del Priore and Cole, unpublished results).

Depletion of *Rss1p* Causes an mRNA Export Defect

Because *RSS1* is an essential gene, we wished to establish the effect on yeast cells caused by loss of *Rss1p* function. Therefore, the *Rss1p* and *Rss1p_{myc}* ORFs were placed under control of the *GAL1* promoter on a *CEN* plasmid and transformed into an *RSS1* null strain, and then *GAL* depletion experiments were performed. Figure 11A shows that in cells lacking the genomic copy of *RSS1* and in which *Rss1p* or *Rss1p_{myc}* expression was driven by the *GAL1* promoter, growth occurred when cells were grown on galactose but not when grown on glucose. Figure 11B shows the growth curves for cells containing *Rss1p* or *Rss1p_{myc}* under control of the *GAL1* promoter and grown in galactose or transferred to glucose-containing media at 37°C. The rate of growth decreased between 10 and 12 h after transfer

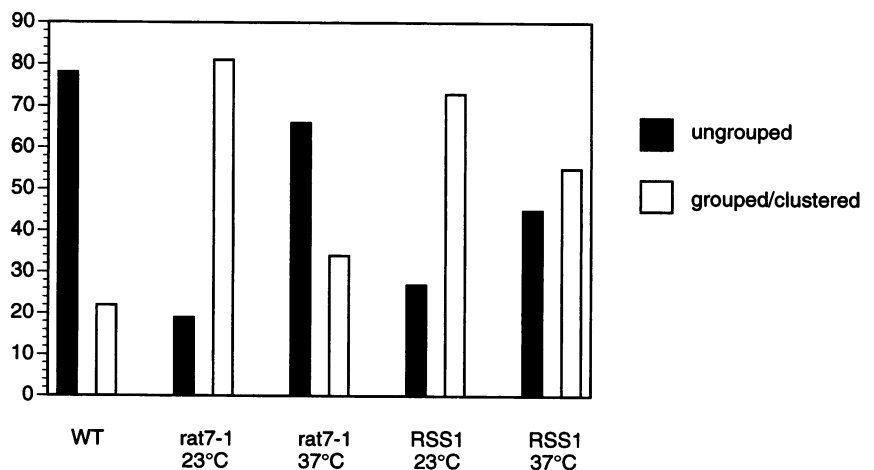


Figure 8. Nuclear pore clustering is partially maintained in *rat7-1* cells overexpressing *RSS1* at 37°C. Electron microscopy was performed on wild-type cells grown at 37°C and on both *rat7-1* and *rat7-1* cells containing a high-copy *RSS1* plasmid, grown at 23°C or shifted to 37°C. Thin sections from 50 different cells were examined for each strain, and the percentage of cells showing ungrouped (filled squares) or grouped/clustered NPCs (open squares) was determined.

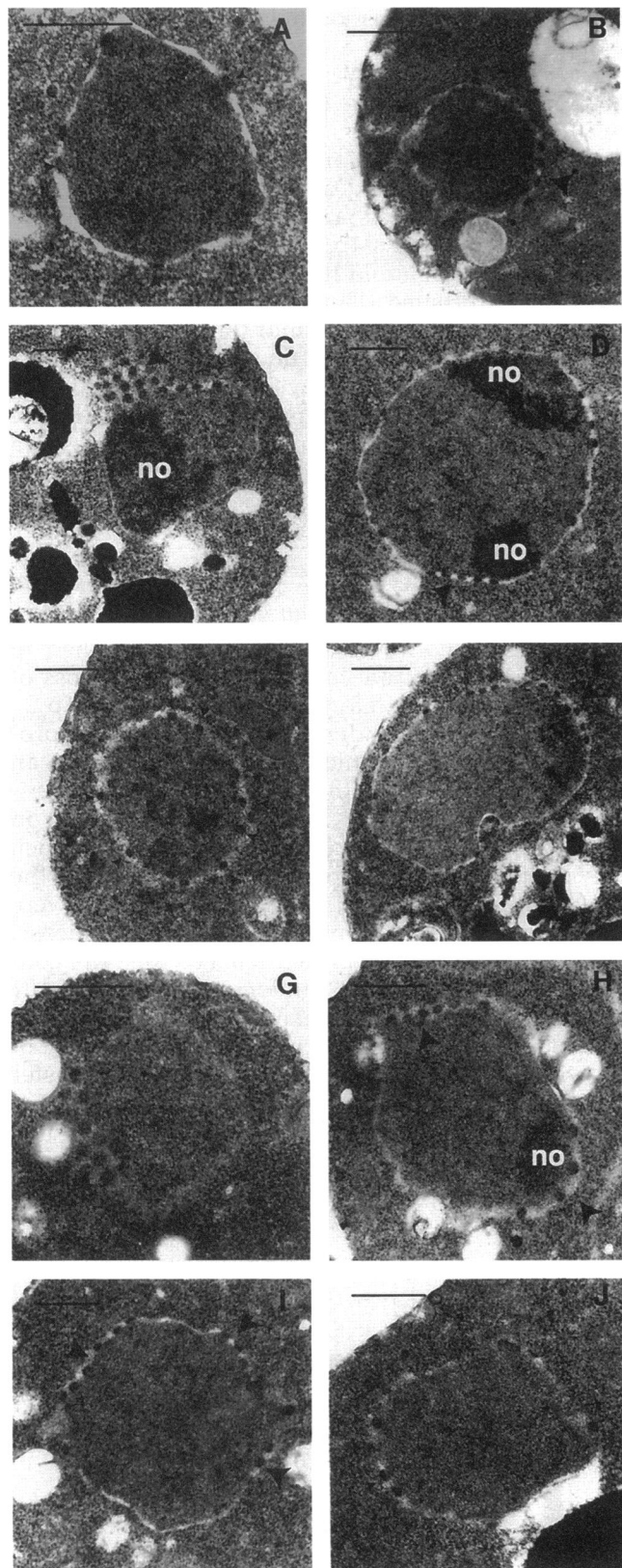


Figure 9.

of cells expressing wild-type Rss1p to glucose and between 6 and 8 h in cells expressing Rss1p_{myc}. The graph suggests that the depletion of Rss1p_{myc} was achieved earlier than the depletion of wild-type Rss1p. This result indicates that myc-tagged Rss1p was less stable than wild-type Rss1p. To monitor the decrease in the levels of Rss1p_{myc} after cells were transferred to glucose, we performed a Western blot on extracts of cells grown on the repressing (glucose) medium for different periods of time (Figure 11C). The figure shows that, within 2.5 h of growth on glucose, the level of the protein was reduced to ~10% of its level in cells grown on galactose. After 5 h of growth on glucose, Rss1p_{myc} was barely detectable, indicating that the protein was readily depleted. Sec13p was used as a control for equal loading.

To determine whether depletion of Rss1p resulted in an mRNA export defect, we performed an in situ hybridization assay in cells expressing Rss1p from the *GAL1* promoter. Cells were grown in galactose or transferred to glucose for 3, 6, 9, or 12 h (Figure 12A). When cells were grown on galactose, poly(A)⁺ RNA was evenly distributed throughout the cell (Figure 12A, 0h), as is the case in wild-type cells. After the cells were grown for 3 h in glucose, no change in the distribution pattern was seen, but after 6 h in glucose, nuclear accumulation of poly(A)⁺ RNA was detectable in ~20-30% of the cells. After 9 h, the percentage of cells accumulating mRNA in their nuclei increased to ~80%. After 12 h in glucose, essentially all cells showed nuclear accumulation of poly(A)⁺ RNA and a substantially reduced cytoplasmic signal. This result provides strong evidence that Rss1p is involved in mRNA export.

Because the strain bearing the *GAL1*-driven myc-tagged *RSS1* plasmid ceased growth more rapidly after transfer to glucose-containing media than cells bearing the *GAL1*-driven wild-type *RSS1* plasmid, we tested whether this was reflected in a more rapid onset of the mRNA export defect by performing an in situ hybridization assay with the *GAL1*-driven myc-tagged *RSS1*-containing strain. Cells grown on galactose were either maintained on galactose or shifted to glucose for 5 h (Figure 12B). Even when grown on galactose, these cells showed some nuclear accumulation of poly(A)⁺ RNA. After 5 h in

Figure 9 (cont). Representative electron micrographs of nuclei showing the different types of NPC distributions seen in wild-type cells incubated at 37°C (A and B), *rat7-1* cells incubated at 23°C (C and D) or shifted to 37°C (E and F), and *rat7-1* cells overexpressing *RSS1* and incubated at 23°C (G and H) or 37°C (I and J). The figure shows examples of evenly distributed (ungrouped), grouped, or clustered NPCs seen in these strains. The large black arrows show examples of grouped or clustered NPCs, and the small black arrows show individual NPCs; no, nucleolus. Bar, 0.5 μm.

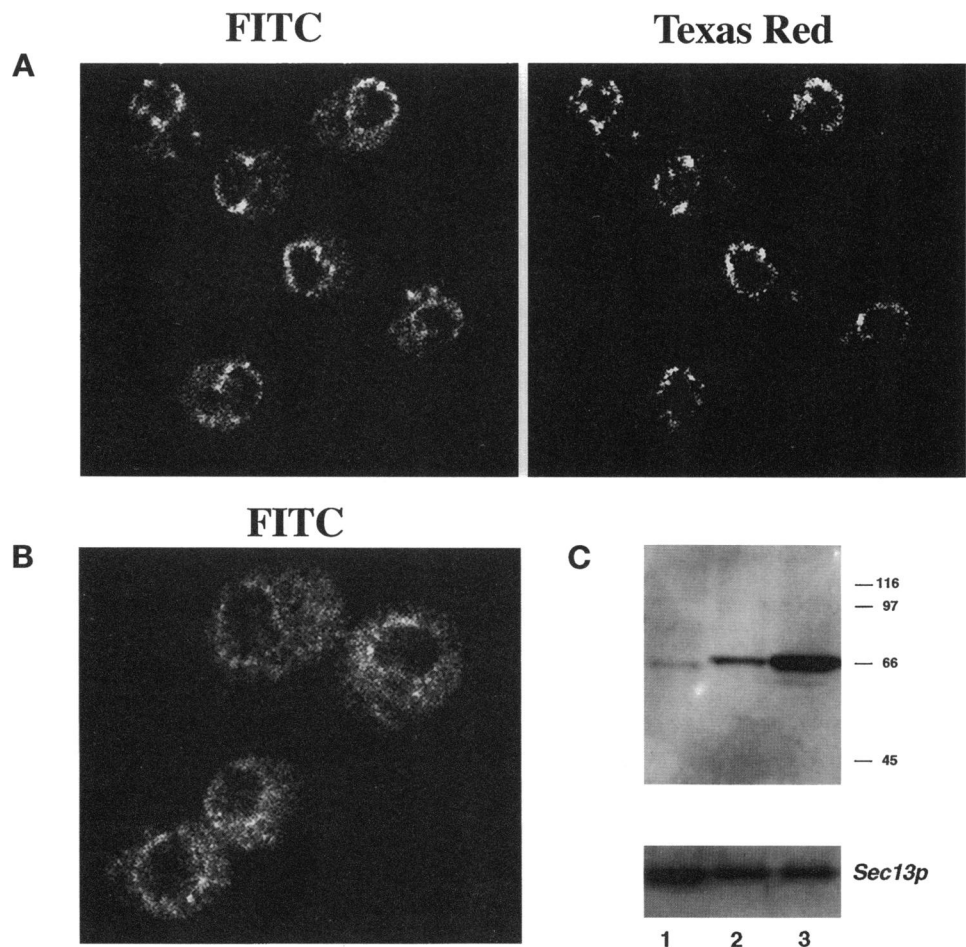
glucose, almost 90% of the cells showed a nuclear mRNA export defect, whereas after 6 h in glucose, the strain bearing the wild-type allele of *RSS1* showed nuclear accumulation in only 20–30% of the cells. These data also suggest that the myc-tagged version of Rss1p is less stable than wild-type Rss1p, such that depletion of this protein occurred earlier, resulting in the more rapid development of the poly(A)⁺ RNA export defect. The lower level of Rss1p_{myc} (compared with wild-type Rss1p) most likely also explains the inability of Rss1p_{myc} to suppress the *rat7-1* mutation.

We also examined nuclear protein import, nuclear pore distribution, and nucleolar integrity in the strain bearing the *GAL1*-driven wild-type *RSS1*. We did not detect any defects in nuclear protein import, nuclear pore distribution, or nucleolar fragmentation, even after 12 h of growth on glucose (our unpublished results). These findings suggest that the defect in mRNA export is the primary defect resulting from depletion of Rss1p.

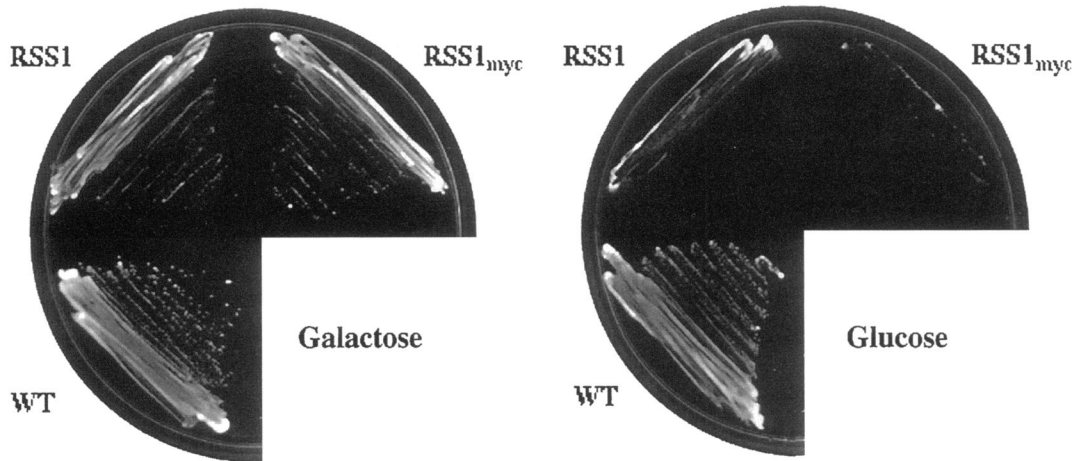
DISCUSSION

In this paper, we describe the identification of the *RSS1* gene by using a screen for high-copy extragenic suppressors of the *rat7-1* allele. *RSS1* encodes a novel 538-amino-acid protein that is located both at NPCs, where it colocalizes with nucleoporins, and within the cytoplasm. By expressing Rss1p from the *GAL1* promoter, Rss1p could be depleted from cells by transferring them from galactose media to glucose media. A defect in export of poly(A)⁺ RNA was observed in almost all of the cells within 9–12 h of transfer to glucose. The kinetics with which growth ceased after transfer to glucose were similar to the kinetics with which cells displayed nuclear accumulation of poly(A)⁺ RNA. No defects in nuclear protein import, nuclear pore distribution, or nucleolar integrity were seen when Rss1p was depleted. Together, these results suggest that Rss1p normally plays a role in nucleocytoplasmic export of poly(A)⁺ RNA.

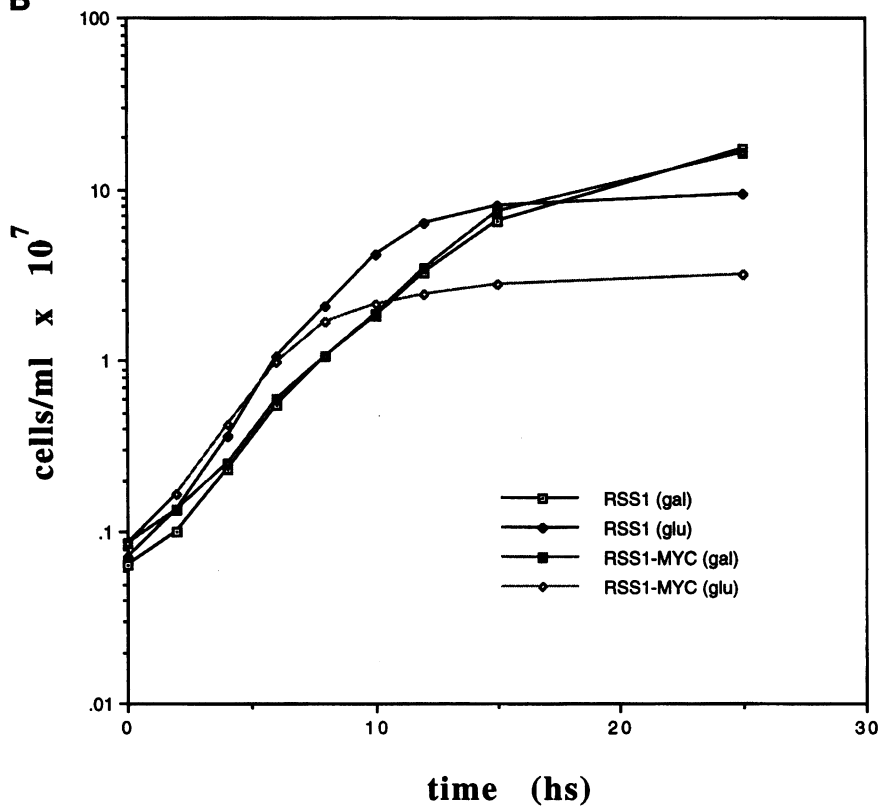
Figure 10. Rss1p localizes to nuclear pore complexes and to the cytoplasm. Immunolocalization of myc-tagged Rss1p was performed. Cells carrying a disruption of *RSS1* were transformed with a *CEN* plasmid encoding myc-tagged Rss1p. Transformed cells were grown to log phase, fixed, and processed for indirect immunofluorescence. Images were taken with a confocal microscope. (A) FITC shows the signal obtained when anti-myc antibody 9E10 was used, and Texas Red shows the signal distribution when the same cells were costained with the RL-1 anti-nucleoporin antibody. (B) Indirect immunofluorescence performed in cells carrying a disruption of *RSS1* and carrying a 2 μ plasmid encoding myc-tagged Rss1p. (C) Western analysis of myc-tagged Rss1p. By SDS polyacrylamide gel electrophoresis, myc-tagged Rss1p migrates at 66 kDa and is overexpressed when produced from a 2 μ vector in the *RSS1* null strain. The anti-myc 9E10 antibody was used to detect myc-tagged Rss1p. (Lane 1) WT (FY86); (lane 2) *rss1 Δ* cells transformed with a *CEN* plasmid encoding myc-tagged Rss1p (VDPY112); (lane 3) *rss1 Δ* cells transformed with a 2 μ plasmid encoding myc-tagged Rss1p (VDPY113). Sec13p was used as a control for equal loading, with an anti-Sec13p antibody obtained from C. Barlowe (Dartmouth Medical School, Hanover, NH).



A



B



C

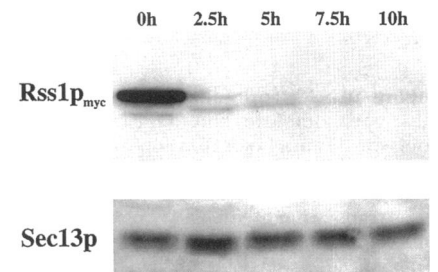


Figure 11. Growth at 37°C of a wild-type yeast culture and of yeast strains disrupted for the chromosomal *RSS1* locus and harboring plasmid-borne *GAL1::RSS1* or *GAL1::RSS1_{myc}* alleles, on galactose or shifted to glucose. (B) Growth curves for the yeast strains shown in A. Cells were grown overnight, diluted to early log phase, and incubated at 37°C either in galactose-containing media or shifted to glucose-containing media at the indicated time. Cell numbers were determined with a hemocytometer. (C) Western analysis of cell extracts prepared from the strain containing the *GAL1::RSS1_{myc}* allele of *RSS1* at various times after transfer to glucose-containing medium. Sec13p was used as a control for equal loading.

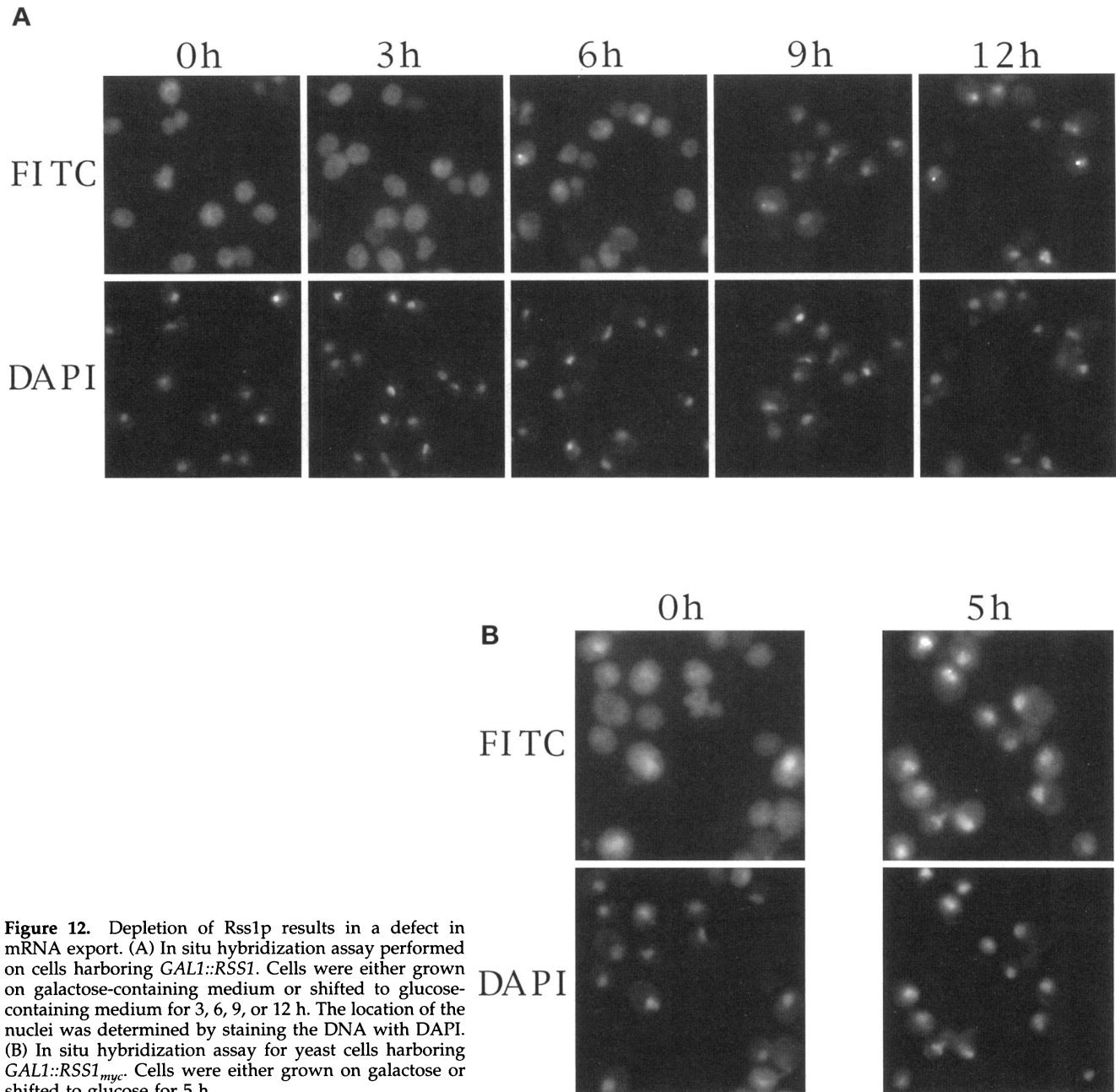


Figure 12. Depletion of Rss1p results in a defect in mRNA export. (A) In situ hybridization assay performed on cells harboring *GAL1::RSS1*. Cells were either grown on galactose-containing medium or shifted to glucose-containing medium for 3, 6, 9, or 12 h. The location of the nuclei was determined by staining the DNA with DAPI. (B) In situ hybridization assay for yeast cells harboring *GAL1::RSS1_{myc}*. Cells were either grown on galactose or shifted to glucose for 5 h.

High-copy *RSS1* suppressed the growth defect of *rat7-1* cells and permitted mutant cells to grow as well at 37°C as they did at 23°C in the absence of the suppressor. However, suppression was only partial, because *rat7-1* cells grew considerably more slowly at 23°C than did wild-type cells (Figure 2), and there was still considerable accumulation of poly(A)⁺ RNA in nuclei. Overexpression of *RSS1* had no deleterious effects on the growth of either wild-type or *rat7-1* cells at 23°C. Suppression was not observed when *RSS1* was expressed from a *CEN* plasmid. On the basis of

Western blot analysis (Figure 8), expression from the high-copy plasmid led to Rss1p levels that were approximately eightfold greater than with the *CEN* plasmid. However, *CEN* plasmids are maintained in yeast cells at ~1-4 copies/cell, and this should result in modest overexpression, as compared with the levels of Rss1p produced from the genomic copy. We estimate that Rss1p was overexpressed by >10-fold when expressed from the high-copy plasmid. The epitope-tagged version of Rss1p seems to have lower stability than the wild-type form, and this most likely explains

the inability of the epitope-tagged form to suppress the *rat7-1* mutation.

In addition to cessation of growth, *rat7-1* cells shifted to 37°C show rapid inhibition of mRNA export, rapid fragmentation of the nucleolus, and a dramatic decrease in rRNA production. We believe that the defects in nucleolar morphology and rRNA biosynthesis are not caused directly by mutation of Rat7p/Nup159p but are most likely indirect consequences of a defect in RNA or ribosome export. Overexpression of *RSS1* partially suppressed all these phenotypes. Although *rat7-1* cells shifted to 37°C for 2 h display virtually no cytoplasmic signal for poly(A)⁺ RNA (Figure 3; Gorsch *et al.*, 1995), the presence of *RSS1* in high copy led to maintenance of a cytoplasmic signal for poly(A)⁺ RNA. This signal could reflect either dramatically reduced turnover of cytoplasmic poly(A)⁺ RNA or continued mRNA export. Only the latter explanation is consistent with the ability of *rat7-1* cells to form colonies at 37°C when *RSS1* is present in high copy. Therefore, we conclude that mRNA export was maintained in *rat7-1* cells shifted to 37°C in the presence of high-copy *RSS1* at a level adequate to support cell growth and division. Although the amount of cytoplasmic mRNA present in *rat7-1* cells suppressed by high-copy *RSS1* was quite low, it is noteworthy that this reduced level was sufficient to support a moderate rate of growth. We have also examined nuclear protein import in *rat7-1* cells through multiple assays, and in all cases, karyophilic proteins were imported efficiently into nuclei (Gorsch *et al.*, 1995; Del Priore and Cole, unpublished results). The fact that *rat7-1* cells show defects in mRNA export but not in nuclear protein import suggests that Rat7p/Nup159p is directly involved in RNA export.

In *rat7-1* cells, Rat7p is lost from the nuclear rim when mutant cells are shifted to 37°C (Gorsch *et al.*, 1995). Because *RAT7/NUP159* is an essential gene, high-copy *RSS1* could be acting to maintain Rat7p at NPCs. However, in the presence of high-copy *RSS1*, the mutant protein was lost from NPCs after a shift to 37°C as rapidly as it was in the absence of high-copy *RSS1* (Figure 6). One of the most novel phenotypes of *rat7-1* cells is that the loss of Rat7p from NPCs in *rat7-1* cells shifted to 37°C is associated with a substantial reversal of the clustering of NPCs seen in these cells grown at 23°C (Gorsch *et al.*, 1995). Interestingly, in the presence of high-copy *RSS1*, most of the clustering and grouping of NPCs seen at 23°C was retained in cells shifted to 37°C, suggesting that maintenance of this clustering may be important for maintaining RNA export.

The data presented in this paper suggest that *RSS1*, in high copy, permits *rat7-1* cells to grow at the non-permissive temperature of 37°C by acting directly to partially suppress the RNA export defect of *rat7-1* cells. Three lines of evidence support the idea that

Rss1p is directly involved in RNA export. First, depletion of *Rss1p* causes a defect in nucleocytoplasmic export of poly(A)⁺ RNA but no defects in nuclear protein import or NPC distribution. Second, *Rss1p_{myc}* was present both in the cytoplasm and at NPCs, a distribution similar to that seen for some factors involved in nucleocytoplasmic transport. Third, when *RSS1* was overexpressed in a *rat7-1* ts strain, it was able to suppress partially the mRNA export defect of this strain.

How Might *Rss1p* Act to Suppress the RNA Export Defect?

An important observation made during these studies is that high-copy *RSS1* is not a bypass suppressor of a null allele of *RAT7/NUP159*. However, all detectable *rat7-1p* was lost from the nuclear rim after a shift of *rat7-1* cells to 37°C, either in the presence or absence of high-copy *RSS1* (Figure 6). Because *rat7-1* cells continue to grow at 37°C in the presence of high-copy *RSS1*, the mutant *rat7-1p* must perform some essential function under these growth conditions. Possibly a very low level of *rat7-1p* remains associated with NPCs after the temperate shift, although none could be detected by indirect immunofluorescence. High-copy *RSS1* could act directly to facilitate RNA export through NPCs lacking detectable *rat7-1p*, or it could act to facilitate limited retention of mutant *rat7-1p* in NPCs. We do not know whether there is a direct interaction between *Rss1p* and Rat7p/Nup159p. Rat7p/Nup159p was readily extracted from NPCs with 100 mM KCl and 0.2% Triton X-100. We were unable to coprecipitate Rat7p/Nup159p and *Rss1p* using these extraction conditions and anti-Rat7p/Nup159p polyclonal antibodies (Del Priore and Cole, unpublished results). Perhaps *Rss1p* does interact with Rat7p/Nup159p, but the interaction may be too weak to survive these mild extraction conditions. Alternatively, *Rss1p* may interact directly with components of the NPC other than Rat7p/Nup159p, or it may interact with non-NPC factors involved in mRNA export.

Two different models can be hypothesized to explain the mechanism of suppression. By one model, *Rss1p* could play a dynamic or enzymatic role in nucleocytoplasmic transport. By conventional fluorescence microscopy, we observed that the nuclear rim staining for *Rss1p_{myc}* was substantially less intense than the cytoplasmic signal. This distribution is similar to that of some of the soluble factors involved in nuclear protein import. For example, importin β /karyopherin β /Kap95p, one of the subunits of the heterodimeric receptor that recognizes nuclear localization signals, is found in the cytoplasm, binds with substrate to NPCs, but does not accumulate in the nucleus (Görlich *et al.*, 1995; Moroianu *et al.*, 1995). The

small GTPase Gsp1p plays a central role in nuclear protein import, and its GTPase activating protein Rna1p is cytoplasmic with a higher concentration near the nucleus (Hopper *et al.*, 1990), a pattern somewhat similar to that of Rss1p. Gsp1p is the yeast homologue of the metazoan Ran protein. One of the yeast Gsp1p-binding proteins Yrb1p also has a distribution similar to that of Rss1p (Schlenstedt *et al.*, 1995). Perhaps NPCs in *rat7-1* cells are not absolutely defective for RNA export, but the rate of export may be too low to support growth of mutant cells. Overexpressed Rss1p might act directly to increase the rate of export through mutant NPCs, thereby restoring growth.

By a second model, *RSS1* overexpression could affect the structure and interactions of NPCs in mutant cells, either by stabilizing a nuclear pore subcomplex that normally contains Rat7p/Nup159p or by maintaining interactions between mutant NPCs and elements of the cytoskeleton or nucleoskeleton that are critical for RNA export. In the absence of Rat7p/Nup159p, a subcomplex of the NPC that contains Rat7p/Nup159p either may not assemble or may not be further assembled into NPCs. Perhaps Rss1p acts to ensure that the other components of a putative Rat7p subcomplex are retained in the pore when mutant *rat7-1p* is lost after a shift to 37°C. NPCs are known to be attached to a nuclear envelope lattice in metazoan cells (Maul, 1977; Goldberg and Allen, 1992; Ris and Malecki, 1993), and there is evidence that a similar attachment occurs in yeast cells (Allen and Douglas, 1989). An association of NPCs with cytoskeletal elements has been observed in metazoan cells (Franke, 1971; Jones *et al.*, 1982), but there is no evidence yet for similar associations in yeast cells. Because Rat7p/Nup159p is located on the cytoplasmic face of NPCs, at a distance consistent with it being part of the cytoplasmic fibrils of the NPC, Rat7p/Nup159p seems more likely to be involved in interactions between NPCs and cytoskeletal elements than with nucleoskeletal elements. Perhaps such interactions are essential for proper transport of substrates through NPCs. If critical connections between NPCs and cytoplasmic structures were disrupted by mutation of the Rat7p/Nup159p nucleoporin, then export substrates might be unable to exit from NPCs and associate with the translation machinery. A significant fraction of polyribosomes, mRNA, and factors required for protein synthesis are associated with the actin cytoskeleton (Lenk *et al.*, 1977; Cervera *et al.*, 1981; Yang *et al.*, 1990; Zambetti *et al.*, 1990a,b; Hesketh and Pryme, 1991; Hansen and Ingber, 1992). Therefore, there may be connections between the cytoskeleton and NPCs, and mRNP exiting the pore may be actively transferred to the actin cytoskeleton or to cytoskeleton-bound ribosomes. Perhaps high-copy Rss1p acts to maintain these NPC-cytoskeletal interactions, thereby permit-

ting *rat7-1* NPCs to retain the ability to export mRNP substrate.

ACKNOWLEDGMENTS

We thank members of the Cole laboratory for helpful discussions and Dr. Erwin Schmidt for support and encouragement during DNA sequence analysis of the portion of chromosome IV containing the *RSS1* gene. We thank C. Barlowe, D. Compton, and C. Heath for critical reading of this manuscript. We also thank C. Barlowe, L. Gerace, M. Snyder, J. Zhu, and J.M. Bishop for antibodies and F. Winston and A. Corbett for yeast strains. Finally, we thank Ken Orndorff and Ann Lavanway for assistance with microscopy. The nucleotide sequence analysis described was supported by the European Union Biotech II Program/Yeast Genome Sequencing Network. All other studies were supported by a grant from the National Institutes of Health (GM-33998) to C.N.C. and by a core grant (CA-16038) to the Norris Cotton Cancer Center, Dartmouth Medical School, Hanover, NH.

REFERENCES

- Aebi, M., Clark, M.W., Vijayraghavan, U., and Abelson, J. (1990). A yeast mutant, *PRP20*, altered in mRNA metabolism and maintenance of the nuclear structure, is defective in a gene homologous to the human gene *RCC1*, which is involved in the control of chromosome condensation. *Mol. Gen. Genet.* 224, 72–80.
- Aitchison, J.D., Blobel, G., and Rout, M.P. (1995). Nup120p: a yeast nucleoporin required for NPC distribution and mRNA transport. *J. Cell Biol.* 131, 1659–1675.
- Akey, C.W. (1990). Visualization of transport-related configurations of the nuclear pore transporter. *Biophys. J.* 58, 341–355.
- Akey, C.W. (1991). Probing the structure and function of the nuclear pore complex. *Semin. Cell Biol.* 2, 167–177.
- Akey, C.W. (1995). Structural plasticity of the nuclear pore complex. *J. Mol. Biol.* 248, 273–293.
- Akey, C.W., and Radermacher, M. (1993). Architecture of the *Xenopus* nuclear pore complex revealed by three-dimensional cryo-electron microscopy. *J. Cell Biol.* 122, 1–19.
- Allen, J.L., and Douglas, M.G. (1989). Organization of the nuclear pore complex in *Saccharomyces cerevisiae*. *J. Ultrastruct. Mol. Struct. Res.* 102, 95–108.
- Amberg, D.A., Goldstein, A.L., and Cole, C.N. (1992). Isolation and characterization of *RAT1*, an essential gene of *Saccharomyces cerevisiae* required for the efficient nucleocytoplasmic trafficking of mRNA. *Genes Dev.* 6, 1173–1189.
- Baudin, A., Ozier-Kalogeropoulos, O., Denouel, A., Lacroute, F., and Cullin, C. (1993). A simple and efficient method for direct gene deletion in *Saccharomyces cerevisiae*. *Nucleic Acids Res.* 21, 3329–3330.
- Bogerd, A.M., Hoffman, J.A., Amberg, D.C., Fink, G.R., and Davis, L.I. (1994). *nup1* mutants exhibit pleiotropic defects in nuclear pore complex function. *J. Cell Biol.* 127, 319–332.
- Byers, B., and Goetsch, L. (1975). Behavior spindles and spindle plaques in the cell cycle and conjugation of *Saccharomyces cerevisiae*. *J. Bacteriol.* 124, 511–523.
- Cervera, M., Dreyfuss, G., and Penman, S. (1981). Messenger RNA is translated when associated with the cytoskeletal framework in normal and VSV-infected cells. *Cell* 23, 113–120.
- Copeland, C.S., and Snyder, M. (1993). Nuclear pore complex antigens delineate nuclear envelope dynamics in vegetative and conjugating *Saccharomyces cerevisiae*. *Yeast* 9, 235–249.

- Davis, L.I. (1995). The nuclear pore complex. *Annu. Rev. Biochem.* 64, 865–896.
- Doye, V., and Hurt, E.C. (1995). Genetic approaches to nuclear pore structure and function. *Trends Genet.* 11, 235–241.
- Doye, V., Wepf, R., and Hurt, E.C. (1994). A novel nuclear pore protein Nup133p with distinct roles in poly(A)⁺ RNA transport and nuclear pore distribution. *EMBO J.* 13, 6062–6075.
- Dworetzky, S.I., and Feldherr, C.M. (1988). Translocation of RNA-coated gold particles through the nuclear pores of oocytes. *J. Cell Biol.* 106, 575–584.
- Elliot, D.J., Stutz, F., Lescure, A., and Rosbash, M. (1994). mRNA nuclear transport. *Curr. Opin. Genet. Dev.* 4, 305–309.
- Fabre, E., and Hurt, E.C. (1994). Nuclear transport. *Curr. Opin. Cell Biol.* 6, 335–342.
- Flach, J., Vogel, J., Bossie, M., Corbett, A., Jinks, T., Willins, D., and Silver, P.A. (1994). A yeast RNA binding protein shuttles between the nucleus and the cytoplasm. *Mol. Cell Biol.* 12, 8399–8407.
- Franke, W.W. (1971). Relationship of nuclear membranes with filaments and microtubules. *Protoplasma* 73, 263–292.
- Gietz, R.D., and Sugino, A. (1988). New yeast-*Escherichia coli* shuttle vectors constructed with in vitro mutagenized yeast genes lacking six-base pair restriction sites. *Gene* 74, 527–534.
- Goldberg, M.W., and Allen, T.D. (1992). High resolution scanning electron microscopy of the nuclear envelope: the baskets of the nucleoplasmic face of the nuclear pores. *J. Cell Biol.* 119, 1429–1440.
- Goldstein, A.L., Snay, C.A., Heath, C.V., and Cole, C.N. (1996). Pleiotropic nuclear defects associated with a conditional allele of the novel nucleoporin Rat9p/Nup85p. *Mol. Biol. Cell* 7, 917–934.
- Görlich, D., Vogel, F., Millas, A.D., Hartmann, E., and Laskey, R.A. (1995). Distinct functions for the two importin subunits in nuclear protein import. *Nature* 377, 246–248.
- Gorsch, L.C., Dockendorff, T.C., and Cole, C.N. (1995). A conditional allele of the novel repeat-containing yeast nucleoporin RAT7/NUP159 causes both rapid cessation of mRNA export and reversible clustering of nuclear pore complexes. *J. Cell Biol.* 129, 939–955.
- Greber, U.F., Senior, A., and Gerace, L. (1990). A major glycoprotein of the nuclear pore complex is a membrane-spanning polypeptide with a large luminal domain and a small cytoplasmic tail. *EMBO J.* 9, 1495–1502.
- Guthrie, C., and Fink, G.R. (1991). Guide to yeast genetics and molecular biology. *Methods Enzymol.* 194, 423–424.
- Hansen, L.K., and Ingber, D.E. (1992). Regulation of nucleocytoplasmic transport by mechanical forces transmitted through the cytoskeleton. In: *Nuclear Trafficking*, ed. C.M. Feldherr, San Diego, CA: Academic Press, 71–86.
- Heath, C.V., Copeland, C.S., Amberg, D.C., Del Priore, V., Snyder, M., and Cole, C.N. (1995). Nuclear pore complex clustering and nuclear accumulation of poly(A)⁺ RNA associated with mutations of the *Saccharomyces cerevisiae* RAT2/NUP120 gene. *J. Cell Biol.* 131, 1677–1697.
- Hesketh, J.E., and Pryme, I.F. (1991). Interaction between mRNA, ribosomes, and the cytoskeleton. *Biochem. J.* 277, 1–10.
- Hinshaw, J.E., Carragher, B.O., and Milligan, R.A. (1992). Architecture and design of the nuclear pore complex. *Cell* 69, 1133–1141.
- Hopper, A.K., Traglia, H.M., and Dunst, R.W. (1990). The yeast RNA1 gene product necessary for RNA processing is located in the cytoplasm and apparently excluded from the nucleus. *J. Cell Biol.* 111, 309–321.
- Iovine, M.K., Watkins, J.L., and Wentle, S.R. (1995). The GLFG repetitive region of the nucleoporin Nup116p interacts with Kap95p, an essential yeast nuclear import factor. *J. Cell Biol.* 131, 1699–1713.
- Izaurrealde, E., and Mattaj, I.W. (1995). RNA export. *Cell* 81, 153–159.
- Jarnik, M., and Aebi, U. (1991). Toward a more complete 3-D structure of the nuclear pore complex. *J. Struct. Biol.* 107, 291–308.
- Jones, J.C.R., Goldman, A.E., Steinert, P.M., Yuspa, A., and Goldman, R.D. (1982). Dynamic aspects of the supramolecular organization of intermediate filament networks in cultured epidermal cells. *Cell Motil.* 2, 197–213.
- Kadowaki, T., Chen, S., Hitomi, M., Jacobs, E., Kumagai, C., Liang, S., Schneider, R., Singleton, D., Wisniewska, J., and Tartakoff, A.M. (1994). Isolation and characterization of *Saccharomyces cerevisiae* mRNA transport-defective (*mtr*) mutants. *J. Cell Biol.* 126, 649–659.
- Kadowaki, T., Schneider, R., Hitomi, M., and Tartakoff, A.M. (1995). Mutations in nucleolar proteins lead to nucleolar accumulation of poly(A)⁺ RNA in *Saccharomyces cerevisiae*. *Mol. Biol. Cell* 6, 1103–1110.
- Kraemer, D.M., Strambio-de-Castillia, C., Blobel, G., and Rout, M.P. (1995). The essential yeast nucleoporin NUP159 is located on the cytoplasmic side of the nuclear pore complex and serves in karyopherin-mediated binding of transport substrate. *J. Biol. Chem.* 270, 19017–19021.
- Lenk, R., Ransom, L., Kaufmann, Y., and Penman, S. (1977). A cytoskeletal structure with associated polyribosomes obtained from HeLa cells. *Cell* 10, 67–78.
- Li, O., Heath, C.V., Amberg, D.C., Dockendorff, T.C., Copeland, C.S., Snyder, M., and Cole, C.N. (1995). Mutation or deletion of the *Saccharomyces cerevisiae* RAT3/NUP133 gene causes temperature-dependent nuclear accumulation of poly(A)⁺ RNA and constitutive clustering of nuclear pore complexes. *Mol. Biol. Cell* 6, 401–417.
- Lupas, A., Van Dyke, M., and Stock, M. (1991). Predicting coiled coils from protein sequences. *Science* 252, 1162–1164.
- Maul, G.G. (1977). The nuclear and cytoplasmic pore complex: structure, dynamics, distribution, and evolution. *Int. Rev. Cytol. Suppl.* 6, 75–186.
- Mehlin, H., Daneholt, B., and Skoglund, U. (1992). Translocation of a specific pre-messenger ribonucleoprotein particle through the nuclear pore studied with electron microscope tomography. *Cell* 69, 605–613.
- Moroianu, J., Blobel, G., and Radu, A. (1995). Previously identified protein of uncertain function is karyopherin A and together with karyopherin B docks import substrate at nuclear pore complexes. *Proc. Natl. Acad. Sci. USA* 92, 2008–2011.
- Nasmyth, K.A., and Tatchell, K. (1980). The structure of transposable yeast mating type loci. *Cell* 19, 753–764.
- Pemberton, L.F., Rout, M.P., and Blobel, G. (1995). Disruption of the nucleoporin gene NUP133 results in clustering of nuclear pore complexes. *Proc. Natl. Acad. Sci. USA* 92, 1187–1191.
- Reichelt, R., Holzenburg, A., Buhle, J., Jarnik, E.L.M., Engel, A., and Aebi, U. (1990). Correlation between structure and mass distribution of the nuclear pore complex and of distinct pore complex components. *J. Cell Biol.* 110, 883–894.
- Rexach, M., and Blobel, G. (1995). Protein import into nuclei: association and dissociation reactions involving transport substrate, transport factors, and nucleoporins. *Cell* 83, 683–692.
- Richardson, W.D., Mills, A.D., Dilworth, S.M., Laskey, R.A., and Dingwall, C. (1988). Nuclear protein migration involves two steps: rapid binding at the nuclear envelope followed by slower translocation through nuclear pores. *Cell* 52, 655–664.

- Ris, H., and Malecki, M. (1993). High-resolution field emission scanning electron microscope imaging of internal cell structures after Epon extraction from sections: a new approach to correlative ultrastructural and immunocytochemical studies. *J. Struct. Biol.* *111*, 148–157.
- Rose, M.D., Winston, F., and Hieter, P. (1989). *Methods In Yeast Genetics*, Cold Spring Harbor, NY: Cold Spring Harbor Laboratory Press.
- Rout, M.P., and Wentle, S.R. (1994). Pores for thought: nuclear pore complex proteins. *Trends Cell Biol.* *4*, 357–365.
- Schlenstedt, G., Wong, D.H., Koepf, D.M., and Silver, P.A. (1995). Mutants in a yeast Ran-binding protein are defective in nuclear transport. *EMBO J.* *14*, 5367–5378.
- Sherman, F. (1991). Getting started with yeast. *Methods Enzymol.* *194*, 3–21.
- Snow, C.M., Senior, A., and Gerace, L. (1987). Monoclonal antibodies identify a group of nuclear pore complex glycoproteins. *J. Cell Biol.* *104*, 1143–1156.
- Traglia, H.M., Atkinson, N.S., and Hopper, A.K. (1989). Structural and functional analysis of *Saccharomyces cerevisiae* wild-type and mutant *RNA1* genes. *Mol. Cell. Biol.* *9*, 2989–2999.
- Unwin, P.N., and Milligan, R.A. (1982). A large particle associated with the perimeter of the nuclear pore complex. *J. Cell Biol.* *93*, 63–75.
- Wente, S.R., and Blobel, G. (1993). A temperature-sensitive *NUP116* null mutant forms a nuclear envelope seal over the yeast nuclear pore complex, thereby blocking nucleocytoplasmic traffic. *J. Cell Biol.* *123*, 275–284.
- Wente, S.R., and Blobel, G. (1994). *NUP145* encodes a novel yeast glycine-leucine-phenylalanine-glycine (GLFG) nucleoporin required for nuclear envelope structure. *J. Cell Biol.* *125*, 955–969.
- Wente, S.R., Rout, M.P., and Blobel, G. (1992). A new family of yeast nuclear pore complex proteins. *J. Cell Biol.* *119*, 705–723.
- Winston, F., Dollard, C., and Ricupero-Hovasse, S.L. (1995). Construction of a set of convenient *Saccharomyces cerevisiae* strains that are isogenic to S288C. *Yeast* *11*, 53–55.
- Wozniak, R.W., Bartnik, E., and Blobel, G. (1989). Primary structure and analysis of an integral membrane glycoprotein of the nuclear pore. *J. Cell Biol.* *108*, 2083–2092.
- Wozniak, R.W., and Blobel, G. (1992). The single transmembrane segment of gp210 is sufficient for sorting to the pore membrane domain of the nuclear envelope. *J. Cell Biol.* *119*, 1441–1449.
- Wozniak, R.W., Blobel, G., and Rout, M.P. (1994). POM152 is an integral protein of the pore membrane domain of the yeast nuclear envelope. *J. Cell Biol.* *125*, 31–42.
- Wright, R., and Rine, J. (1989). Transmission electron microscopy and immunocytochemical studies of yeast: analysis of HMG-CoA reductase overproduction by electron microscopy. *Methods Cell Biol.* *31*, 473–512.
- Yang, F., Demma, M., Warren, V., Dharmawardhane, S., and Condeelis, J. (1990). Identification of an actin-binding protein from *Dictyostelium* as elongation factor 1. *Nature* *347*, 494–496.
- Zambetti, G., Fey, E.G., Penman, S., Stein, J., and Stein, G. (1990a). Multiple types of mRNA-cytoskeletal interactions. *J. Cell Biol.* *44*, 177–187.
- Zambetti, G., Wilming, L., Fey, E.G., Penman, S., Stein, J., and Stein, G. (1990b). Differential association of membrane-bound and non-membrane-bound polysomes with the cytoskeleton. *Exp. Cell Res.* *191*, 246–255.